

AD-A190 092

AN OVERVIEW OF GRAIN GROWTH THEORIES FOR PURE SINGLE  
PHASE SYSTEMS (U) ATOMIC ENERGY RESEARCH ESTABLISHMENT  
HARWELL (ENGLAND) H U ATKINSON OCT 86 AERE-R-12136

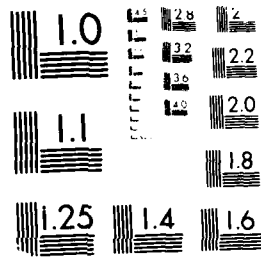
1/1

UNCLASSIFIED

F/C 28/2

ML

END  
78



MICROCOPY RESOLUTION TEST CHART  
1.0 1.1 1.25 1.4 1.6 1.8 2.0 2.2 2.8 3.2 3.6 4.0

AERE R 12136

APPROVED FOR PUBLICATION

AERE R 12136

THIS DOCUMENT IS INTENDED FOR PUBLICATION IN THE OPEN LITERATURE. Until it is published, it may not be circulated, or referred to outside the organisation to which copies have been sent.



AD-A190 092

United Kingdom Atomic Energy Authority

**HARWELL**

**An overview of grain growth theories for pure single phase systems**

H V Atkinson

**DTIC**  
**ELECTE**  
JAN 1 1 1988  
**S** **D**  
D

**COPYRIGHT AND REPRODUCTION**  
Enquiries about copyright and reproduction should be addressed to the Publications Office, AERE Harwell, Oxfordshire, England OX11 0RA.

**EXEMPTION CERTIFICATE**  
Exempted from public release,  
Distribution Unlimited

Materials Development Division  
Harwell Laboratory, Oxfordshire OX11 0RA

October 1986

APPROVED FOR PUBLICATION

C16

87 12 20 1988

AN OVERVIEW OF GRAIN GROWTH THEORIES  
FOR PURE SINGLE PHASE SYSTEMS

H.V. Atkinson

ABSTRACT

The development of theories for normal grain growth in pure single phase systems is reviewed. A major theme which emerges is the interplay between the topological requirements for space filling and the kinetics of change in mean grain size with time. Computer simulation is now playing a key role in exploring this interplay.

Materials Development Division  
Harwell Laboratory

October 1986

HL86/1409 (C16)

SEARCHED	INDEXED
SERIALIZED	FILED
OCT 1986	
A-1	



CONTENTS

	<u>Page No.</u>
1. INTRODUCTION	1
2. PARABOLIC GRAIN GROWTH KINETICS	3
2.1 The Burke and Turnbull Analysis	3
2.2 Experimental Results	5
3. TOPOLOGICAL REQUIREMENTS	7
4. MEAN FIELD THEORIES	11
4.1 Theories Concentrating on the Drift-Velocity Term	12
4.1.1 Hillert's Analysis	13
4.1.2 Feltham's Analysis	13
4.2 Louat's Theory Concentrating on the Diffusion Term	14
5. GRAIN GROWTH AS DISLOCATION CLIMB	16
6. THE RHINES AND CRAIG TOPOLOGICAL ANALYSIS OF GRAIN GROWTH	17
6.1 The Sweep Constant	18
6.2 Structural Gradient	18
6.3 Analysis for Grain Growth Kinetics	19
6.4 Comparison of Mean Grain Intercept and $(V)^{1/3}$ Methods	21
6.5 Analysis of Grain Growth Kinetics Continued	22
6.6 Steady State Conditions	22
6.7 Summary and Discussion of the Rhines and Craig Analysis	23
7. TOPOLOGICAL CHARACTERISTICS OF THE STEADY STATE	25
7.1 Monte-Carlo Simulations to Obtain Distributions of Topological Parameters	25
7.2 Analytical Method to Obtain $f_n$	26
8. KURTZ AND CARPAY STATISTICAL THEORY OF NORMAL GRAIN GROWTH	28
8.1 Analysis	28
8.2 Experimental Results	31
9. STRUCTURE OF RANDOM CELLULAR NETWORKS	32
9.1 Lewis' Law	32
9.2 Asymptotic Evolution of 2-D Soap Froth	34
9.3 The Aboav-Weaire Law	35
9.4 Maximum Entropy Considerations	36
9.5 Topological Properties of Trivalent Cellular Structures	39

CONTENTS - continued

10. COMPUTER SIMULATION OF GRAIN GROWTH	41
10.1 Novikov's Model	41
10.2 Linear Bubble Growth Model	43
10.3 2-D Soap Froth Simulation	44
10.4 Simulation of 2-D Grain Growth using the Classical Boundary Migration Equation	48
10.5 Monte-Carlo Simulations of Grain Growth	49
10.5.1 2-D	49
10.5.2 3-D	52
11. SUMMARY	53

ACKNOWLEDGEMENTS

REFERENCES

TABLES

Table 1	Kinetics of grain growth for various mechanisms (from Brook (1976)).
Table 2	Grain growth exponents for isothermal grain growth in metals (from Anderson et al. (1984)).

ILLUSTRATIONS

Fig. 1	Typical 2-D section through a 3-D grain structure (after Underwood (1970)). The 4-rayed vertex will tend to decompose into two three-rayed vertices as growth occurs.
Fig. 2	Schematic representation of grain boundary velocity $v_g$ as a function of driving force for (a) pure material, (b) impure material not exhibiting breakaway, (c) impure material exhibiting breakaway at $F_{C1}$ , (d) highly impure material exhibiting breakaway at $F_{C2}$ (from Bauer (1982)).
Fig. 3	2-D grain structure illustrating instability when the array does not consist only of regular hexagons (after Hillert (1965)).
Fig. 4	A group of regular tetrakaidecahedra (after Smith (1952))

- Fig. 5 Section through a tetrakaidecahedron showing the deviation from equilibrium angles (after Doherty (1984)).
- Fig. 6 (a) Number of grains versus grain size.  
(b) Grain size distributions.
- Fig. 7 (a) The grain size distribution function from computer simulation (histogram) (see Section 10.4) compared with three theoretical distributions: the log-normal (solid) and those proposed by Hillert (1965) (dotted) and Louat (1974) (dashed) (after Srolovitz et al. (1984)).  
(b) The grain size distribution function from computer simulation (histogram) (see Section 10.4) compared with a log-normal fit to experimental data of Beck (1954) for Al (solid curve) and Aboav and Langdon (1969) for MgO (dashed curve) (after Srolovitz et al. (1984)).
- Fig. 8 Plot of  $M_v S_v$  versus  $N_v$  for steady state grain growth in Al (after Rhines and Connell (1974)).
- Fig. 9 Plot of grain volume ( $1/N_v$ ) against time of annealing for aluminium showing a linear relationship (after Rhines and Craig (1974)).
- Fig. 10 Schematic representation of grain transfer between topological classes in a fixed time interval. The transfer of larger grains to the next lower class results in a continuous growth in the mean diameter in the classes with  $F < \bar{F}$  even though all the individual grains in these classes are collapsing due to surface tension constraints. The transfer rates are greatest in the lowest classes (after Kurtz and Carpay (1980)).
- Fig. 11 Schematic diagram illustrating that as a 3-sided grain shrinks adjacent grains gain in diameter in inverse proportion to their diameter.
- Fig. 12 Voronoi construction for random points (after Weaire and Rivier (1984)).
- Fig. 13 Illustration of a fractal structure for a soap cell system (after Weaire and Rivier (1984)).
- Fig. 14 The generalized grain growth model in Hunderi and Ryum (1979). Only contacts activated from grain  $i$  are shown. The process is repeated for all grains.
- Fig. 15 Sample microstructure on a triangular lattice where integers denote orientation and lines represent grain boundaries (after Anderson et al. (1984)).
- Fig. 16 The growth rate of individual grains in normalized grain size space,  $d(R/\bar{R})/dt$  versus  $R/\bar{R}$  (after Srolovitz et al. (1984)).

## 1. INTRODUCTION

Grain growth is the process by which the mean grain size of an aggregate of crystals increases. The driving force for this results from the decrease in free energy which accompanies reduction in total grain boundary area. Given a sufficiently high temperature and no factors which impede grain boundary migration, a polycrystal will evolve towards a single crystal. In reality, this goal is rarely attained.

All natural structures (and many artificial ones) represent some compromise between order and chaos. Grain boundary networks in metallurgical and ceramic polycrystals have features in common with soap froths, arrays of biological cells, geographical and ecological territories and other natural structures (Weaire and Rivier (1984)). Microstructure of polycrystalline materials is also a key factor technologically, determining a wide range of properties including mechanical strength, toughness, electrical conductivity and magnetic susceptibility. Understanding of grain growth is thus of fundamental importance, not only for its intrinsic interest and wider ramifications for insight into other natural phenomena, but also for its technological significance. It is, however, proving an elusive and challenging target, as will become apparent in this review.

The review deals with "normal" grain growth, which is observed in a wide variety of materials ranging from pure metals to complex alloys and inorganic ceramics. It is generally defined as having two main attributes:-

- (1) **Uniform Appearance** - There is a relatively narrow range of grain sizes and shapes.
- (2) **Scaling** - A simple change in scale is sufficient to make the distributions of sizes at two widely separated points in time coincide with each other, i.e. the form of the distribution is time-invariant.

Normal growth contrasts with abnormal grain growth (sometimes called secondary recrystallisation) in which a few large grains develop and



consume a matrix of smaller ones, eventually impinging and reverting to normal growth.

In this overview, the development of theories for normal grain growth will be examined. A major theme which will emerge is the interplay between the topological requirements for space filling and the kinetics of change in mean grain size with time. Computer simulation is now playing a key role in exploring this interplay.

The review follows through the historical development of the subject from the early 1950's onwards. In this way it is possible to introduce the important concepts in a digestible form for those not already fully conversant with the literature on grain growth theories. The aim is to clarify issues in the breadth of this complex subject for the materials scientist.

The structure of the overview is as follows. In Section 2, Burke and Turnbull's simple dimensional argument to obtain parabolic grain growth kinetics from consideration of the driving forces on an isolated section of grain boundary is presented and experimental results, which in general deviate from the parabolic law, are discussed. Topological requirements for space-filling by grains are examined in Section 3 and the contribution of topological transformations to growth brought out. Early mean field theories, in which the behaviour of a grain embedded in an averaged environment is considered, are discussed in Section 4, and in Section 5 a view of grain growth as dislocation climb is indicated, tying in with the topological transformations first described in Section 3. Section 6 treats the important Rhines and Craig (1974) topological analysis of grain growth, bringing in their concepts of the sweep constant and the structural gradient, and showing how these authors obtained a cubic rather than parabolic grain growth law. These contrasting laws are discussed and some attention is given to the problem of deducing 3-D parameters from 2-D sections. In Section 7, two models to predict distributions of topological parameters in the steady-state are described, and in Section 8, Kurtz and Carpay's (1980a, 1980b) statistical theory, which divides the grains into topological classes and examines the time evolution in each class, is discussed. Random cellular networks can be used to model grain boundary networks.

and the latest thoughts in the literature are outlined in Section 9, including:- the applicability of Lewis' Law connecting the mean grain area of n-sided grains to n; the asymptotic behaviour (or otherwise) of 2-D soap froths (soap froths often being presented as a model for grain growth phenomena); the Aboav-Weaire Law for correlation between the number of sides of a grain and the average number of sides of its neighbours; maximum entropy arguments to predict the most probable distributions of cell (or grain) sizes and shapes; and the topological properties of trivalent structures. In Section 10, the recent computer simulations of grain growth by various groups are discussed.

## 2. PARABOLIC GRAIN GROWTH KINETICS

### 2.1 The Burke and Turnbull Analysis

In a classic paper of the early 1950's, Burke and Turnbull (1952) deduced a parabolic relationship for grain growth kinetics. They modelled migration of a boundary as occurring by atom transport across the boundary under a pressure due to surface curvature. They considered the forces on an isolated section of boundary due to surface curvature alone. The boundary tends to migrate towards its centre of curvature as this reduces the area of boundary and hence the energy associated with it. The velocity  $v$  for a pure material is such that

$$v = \mu P \quad (1)$$

where  $\mu$  is the mobility, the velocity under unit pressure  $P$ . Using reaction rate theory, Burke and Turnbull deduced that

$$\mu = \frac{bv\Omega}{k_B T} \exp\left(\frac{-\Delta G_b}{k_B T}\right) \quad (2)$$

where  $b$  is the atomic diameter,  $v$  the atomic vibration frequency,  $k_B$  Boltzmann's constant,  $T$  absolute temperature and  $\Delta G_b$  the activation energy for migration of an atom across the boundary. This expression is not necessary for the deduction of parabolic kinetics, except in that it is important to postulate that the mobility,  $\mu$ , is not dependent on the grain size. It represents however, one of the first steps in thinking

about boundary migration mechanisms, a whole parallel area of research with that into grain growth theories.

The pressure P:

$$P = \gamma \left( \frac{1}{r_1} + \frac{1}{r_2} \right) \quad (3)$$

where  $\gamma$  is the grain boundary free energy and  $r_1$  and  $r_2$  the principal radii of curvature of the surface. Assuming the boundary is part of a sphere,  $r = r_1 = r_2$ . Burke and Turnbull then made four assumptions in order to find the dependence of the mean grain size of any array of grains on time:-

- (1)  $\gamma$  is independent of grain size and time, and the same for all boundaries.
- (2)  $r$ , the radius of curvature, is proportional to  $\bar{R}$ , the mean grain radius:  $r = C_1 \bar{R}$  where  $C_1$  is a constant.
- (3)  $\frac{dR}{dt}$  is proportional to P (i.e.  $\mu$  is independent of R, and  $\frac{dR}{dt}$  is proportional to the velocity  $v$ ):  $\frac{dR}{dt} = C_2 P$  where  $C_2$  is a constant.

and crucially,

- (4) the only forces which act on any grain boundary in the array are those due to surface curvature.

Hence,

$$\frac{dR}{dt} = \frac{2C_2 \gamma}{C_1 \bar{R}}$$

Then, if  $R = \bar{R}$ ,

$$\bar{R}_t^2 - \bar{R}_0^2 = \frac{4C_2 \bar{r} t}{C_1}$$

and hence,

$$\bar{R}_t^2 - \bar{R}_0^2 = Kt \quad (4)$$

where  $\bar{R}_t$  is the mean grain size at time  $t$ ,  $\bar{R}_0$  the initial mean grain size and  $K$  a constant. This is the parabolic grain growth equation and should be valid for both 3-D and 2-D. In the limit where  $R_t \gg R_0$ ,

$$\bar{R}_t^2 = Kt \quad (5)$$

and

$$R_t = Kt^{1/n} \quad \text{where } n = 2 \quad (6)$$

$n$  is often termed the grain growth exponent. (It should be distinguished from the  $n$  used to denote the number of edges surrounding a grain, which will enter later.)

## 2.2 Experimental Results

Since the parabolic law for grain growth kinetics was deduced, experimentalists have devoted much effort to extracting grain growth exponents and then making declarations about how far their samples approach the ideal epitomised by  $n = 2$ . This tendency has been further encouraged by schemes to identify a variety of different values of  $n$  with different factors controlling grain growth. These are summarised in Table 1 (from Brook 1976). The most commonly observed value, 3, (e.g. see Anderson et al (1984)) can for example be indicative of any of five separate processes. Any attempt to isolate controlling mechanisms must involve investigation not only of the grain growth kinetics and activation energy (which can sometimes be identified with a controlling mechanism such as grain boundary or surface diffusion) but also microstructural and compositional parameters (pore size and

distribution, extent of solid second phases, level of dopants and their segregation). In addition, it will become clear that this approach is to be questioned until further advances in grain growth theory, both in pure single phase materials, and in those containing impurities, particles and pores, are made.

Experimental values for the growth exponent for zone-refined metals in which impurity levels are very low (a few ppm or less), are given in Table 2. The values vary from  $n = 2$  to  $n = 4$  with an average of  $2.5 \pm 0.4$ . They are almost invariably obtained from analysis of 2-D sections through the microstructure, the mean grain diameter being obtained by finding the average linear intercept. To find the average mean intercept, a line length  $L$  is drawn across the microstructure, the number  $\lambda$  of intercepts with grain boundaries counted, and  $L/\lambda$  calculated. This procedure is repeated with the line drawn at random orientations and the mean  $L/\lambda$  found. A typical 2-D section through a 3-D network is shown in Fig.1. The important issue of the relationship between 2-D sections and 3-D structures will be returned to in Section 6.

Martin and Doherty (1976) have reviewed grain growth exponents for zone-refined metals. In their view,  $n > 2$  can be attributed to

(i) solute drag (even for zone-refined metals) giving rise to a non-linear dependence of velocity  $v$  on driving force  $P$  (see Fig. 1)

or

(ii) 
$$\text{velocity } v = \mu [P - P_0] \quad (7)$$

where  $P$  is the minimum driving force below which no migration can occur (Grey and Higgins (1972, 1973)). Martin and Doherty (1976) favour the latter explanation because in grain growth, where the driving force is lower than for recrystallisation, the velocity is expected to remain within the low velocity regime of Fig. 2. However, this conclusion relies on the assumption that  $n = 2$  for a pure, ideal single phase system.

The key questions to arise from the Burke and Turnbull analysis are therefore:

- (1) what causes departures from  $n = 2$  in relatively pure single phase materials?

or alternatively,

- (2) is  $n = 2$  to be expected i.e. is the Burke and Turnbull approach adequate?

In summary, Burke and Turnbull analysed the expected migration rate of a single portion of boundary and assumed their expression represented the mean behaviour of a whole array of grains.

### 3. TOPOLOGICAL REQUIREMENTS

C.S. Smith (1952) produced the second classic paper of the early 1950's (see also C.S. Smith, (1953), (1954), (1964a,b)). He emphasised that "Normal grain growth results from the interaction between the topological requirements of space-filling and the geometrical needs of surface tension equilibrium." Smith enumerated the topological requirements in some detail. They are summarized here for those not familiar with space-filling criteria.

In both 2-D and 3-D, the structure consists of vertices joined by edges (also termed 'sides') which surround faces (see Fig. 1). In the 3-D case, the faces surround cells. The cells, faces, edges and vertices of any cellular structure obey the conservation law (Euler's equation), provided the face or cell at infinity is not counted:

$$F - E + V = 1 \quad \text{2-D plane} \quad (8)$$

$$-C + F - E + V = 1 \quad \text{3-D Euclidean space} \quad (9)$$

Here C is the number of cells, E of edges, F of faces and V of vertices.

The number of edges joined to a given vertex is its coordination number  $z$ . For topologically stable structures, i.e. those in which the topological properties are unchanged by small deformations,  $z = 3$  (2-D) and  $z = 4$  (3-D) everywhere. For 2-D this can be illustrated by a 4-rayed vertex, which will tend to be unstable and to decompose into a two 3-rayed vertices (see Fig.1. inset). This transformation has been termed "neighbour-switching" by Ashby and Verrall (1973). For a 2-D structure, in which all the boundaries have the same surface tension, the equilibrium angles at a vertex are  $120^\circ$ . The tetrahedral angle,  $109^\circ 28'$ , is the equilibrium angle at a four-edged vertex in 3-D.

An immediate consequence of Euler's equation in 2-D, for an equilibrium structure ( $z = 3$ ), is that the average number of edges,  $\langle n \rangle$ , surrounding a cell (here referring to 2-D faces as cells in accordance with general usage) is 6, in the limit of a large system, i.e.

$$\langle n \rangle = 6 \quad (2-D) \quad (10)$$

Since three edges meet at every vertex and each edge joins two vertices,

$$2E = 3V \quad (2-D) \quad (11)$$

As every edge joins two faces,

$$\sum n f_n = 2E \quad (2-D) \quad (12)$$

where  $f_n$  is the number of  $n$ -sided cells.

Grain growth in 2-D is inevitable unless a structure consists of an absolutely regular array of hexagons. If even one 5-sided polygon is introduced into an array (and it has to be balanced by a 7-sided one to maintain  $\langle n \rangle = 6$ ) then the sides of the grains must become curved in order to maintain  $120^\circ$  angles at the vertices (see Fig. 3). Grain boundary migration then tends to occur because of the curvature, in order to reduce boundary surface area. Any grain with  $n > 6$  will tend to grow because its boundaries are concave (and boundaries migrate towards their centre of curvature). Grains with  $n < 6$  will tend to

shrink as they have convex sides. In Fig.3, the shrinkage of the 5-sided grain leads to a 4-rayed vertex in b). This decomposes into two 3-rayed vertices in c) and the 5-sided grain becomes 4-sided. The grain continues to shrink and undergoes a similar transformation to become 3-sided (see d), e)). It then shrinks away completely leaving a 5-sided grain neighbouring a 7-sided grain in f), as in a).

For a 3-D array where all vertices have  $z = 4$ , the equivalent relations to those given above for 2-D are

$$\langle f \rangle = \frac{12}{6 - \langle n \rangle} \quad (13)$$

$$E = 2V \quad (14)$$

$$\sum nF_n = 3E \quad (15)$$

where  $\langle f \rangle$  is the average number of faces for 3-D cells and  $\langle n \rangle$  is the average number of sides per face in the cell. Most random structures have  $\langle f \rangle \approx 14$  but this is not an exact result. There is no regular polyhedron with plane sides which has exactly the tetrahedral angle  $109^\circ 28'$  between its edges. The nearest approach to space filling by a regular plane-sided polyhedron in 3-D is obtained with Kelvin tetrakaidecahedra spaced on a body centred cubic lattice (see Fig. 4). Even with tetrakaidecahedra, the angles are not exactly those required (see Fig. 5) and boundaries must become curved to obtain equilibrium at the vertices. Grain growth then follows. In general, grains tend to be arranged randomly rather than with their centres on a regular lattice and also grain sizes vary. In such a random array, Smith (1952) asserted that, for an array containing  $N$  cells:- the average number of vertices/cell ( $V/N$ )  $\rightarrow 6$ ; the average number of faces/cell  $\rightarrow 7$ ; and the average number of edges/face  $\rightarrow 36/7$ . He suggested  $(6 - V/N)$  as a criterion of additional surface area in the system and therefore of "tendency" to grain growth.

C.S. Smith elegantly illustrated the topological principles given above using soap froths. Wesire and Rivier (1984) have discussed the extent to which soap froths can be used to model grain growths in



polycrystals. In both systems, a driving force for reduction in surface energy causes boundaries to migrate to reduce boundary area. In soap froths, each cell contains a fixed volume of gas and molecules permeate through the cell membranes to equalise pressures in adjacent bubbles. In polycrystalline grain growth, atoms must also be transferred across the boundary but, in contrast with soap froths:-

- (1) boundary energy may vary with orientation.
- (2) transport of vacancies along the boundary may contribute to the migration process by supplying vacancies to enable diffusion of atoms across the boundary by a vacancy mechanism.
- (3) polycrystalline aggregates tend to be much further from equilibrium at a given time because diffusion processes to attain equilibrium in solids are slow in comparison with those in a gas/liquid soap froth system, i.e. the gas has a zero shear modulus.

This discussion will be returned to in Section 9.2.

Von Neumann (1952), in a note at the end of the C.S. Smith paper, argued, on the basis of surface tension requirements, that in 2-D, the rate of growth of a cell is proportional to its number of sides minus 6. Rivier (1983) showed that this is in fact a geometrical result and not due to surface tension. Von Neumann's law is to be discussed again in Section 9.1.

It is worthy of note that C.S. Smith also stated, "In a large array, with a random distribution of sizes, there is probably a tendency toward a fixed distribution of shapes and relative cell sizes determined by topological requirements and by the equation for rate of volume change as a function of curvature." The question of whether there are characteristic distributions for cell sizes and shapes has been the basis for much debate and will be discussed in subsequent sections. In analyses of grain growth kinetics, distributions have been:-

- (1) Assumed by Feltham (1957), Novikov (1978) and Kurtz and Carpay (1987a).
- (2) Predicted by analysis by Hillert (1965) and Louat (1974)).
- (3) Predicted by computer simulation by Weaire and Kermode (1983a,b, 1984), Anderson et al. (1984) and Srolovitz, et al. (1984a).

In summary, at the end of this Section, Smith was one of the first to recognize the importance of topological space-filling requirements and their influence on grain growth, but told us nothing about how quickly topological transformations and overall grain growth can occur. In contrast, Burke and Turnbull examined the kinetics of migration of an isolated spherical grain but did not attempt to find how the fact that it is connected into a space-filling network governs its migration. We shall now start to examine the evolution of theories aimed at binding these two approaches together. In the next section we shall look at the early "mean field theories" in which the growth of a grain embedded in an average environment is examined. These followed on from the Burke and Turnbull analysis.

#### 4. MEAN FIELD THEORIES

The mean field approach deals with the change in size of an isolated grain embedded in an environment which represents the average effect of the whole array of grains. It was initially developed by Feltham (1957), Hillert (1965) and Louat (1974). Hunderi and Ryum (1980) gave the basis for describing how these theories can be classified. This can be explained as follows. During normal grain growth, there is an increase in the mean grain size and a decrease in the number of grains in the system. This process may be viewed as the change of the grain size distribution  $f(R)$  with time (see Fig. 6). Consider grains of a given size  $R$ . These can be seen to be changing size as the result of:

- (1) A diffusion-like process in which grains larger than  $\bar{R}$  get

larger due to the "concentration gradient"  $\frac{df}{dR}$  (see Fig. 6(b) showing grain entering and leaving the size class  $R_1$  along the R axis).

- (2) A velocity  $v = dR/dt$  due to a driving force (assumed to be reduction in boundary curvature); grains are entering and leaving the size class  $R_2$  along the time axis.

The physical basis for the diffusion-like process is not clear. The overall flux  $j$  of grains is given by

$$j = -D \frac{\partial f}{\partial R} + fv \quad (16)$$

where  $D$  can be identified with a diffusion coefficient which only depends on the specific grain boundary mobility and  $f$  is the distribution function which is a function of both  $R$  and  $t$  and can therefore be written  $f(R,t)$ . The continuity of the flux is then:

$$\frac{\partial f}{\partial t} = \frac{\partial}{\partial R} (-j) = \frac{\partial}{\partial R} (D \frac{\partial f}{\partial R}) - \frac{\partial}{\partial R} (fv) \quad (17)$$

#### 4.1 Theories Concentrating on the Drift-Velocity Term

Feltham (1957) and F. Lert (1965) assumed, more or less implicitly, that the drift due to a driving force dominates normal grain growth and that the driving force is related to elimination of grain boundary area. The first term in the right hand side of (17) is therefore neglected:

$$\frac{\partial f}{\partial t} + \frac{\partial}{\partial R} (fv) = 0 \quad (18)$$

There are then two possible approaches to obtaining a mean growth rate,

- (1) Using a particular expression for the drift velocity  $v$ , solve for  $f(R,t)$ , the grain size distribution.

(2) Using an experimentally determined  $f$ , find  $v$ .

Hillert (1965) adopted the first approach and Feltham (1957) the second.

#### 4.1.1 Hillert's Analysis

Hillert suggested an expression for the drift velocity  $v$  (seen as equivalent to the boundary velocity and proportional to  $dR/dt$ ) such that

$$v = \alpha \mu \gamma \left( \frac{1}{R_{\text{crit}}} - \frac{1}{R} \right) \quad (19)$$

where  $\alpha$  is a geometric factor,  $\mu$  the mobility of the boundary,  $\gamma$  the surface energy of the boundary, and  $R_{\text{crit}}$  a critical grain size which varies with time.  $\mu$  and  $\gamma$  are assumed independent of  $R$ .  $R_{\text{crit}}$  is such that if  $R > R_{\text{crit}}$  the grain will grow, and if  $R < R_{\text{crit}}$  it will shrink. Using (19), the kinetics become identical with those for Ostwald ripening of a distribution of second phase particles with interphase reactions controlling the rate at which large particles grow at the expense of smaller ones. Hillert used previous analyses of Ostwald ripening to obtain parabolic kinetics for grain growth, i.e. equation (4). He also solved for a distribution function of  $f(R,t)$ , which proved to be quite sharply peaked in comparison with a log-normal distribution (see Fig. 7(a)). The log-normal distribution is often fitted to experimental data (Fig. 7(b)) but is not an entirely satisfactory distribution, as will be discussed below.

#### 4.1.2 Feltham's Analysis

Feltham (1957), on the other hand, asserted that the experimental distribution  $f(R,t)$  is log-normal (i.e. frequency versus  $\log$  (grain-size) gives a Gaussian distribution), and time-invariant if plotted against  $R/\bar{R}$  where  $\bar{R}$  is the mean grain size.

Feltham solved for the velocity  $v$ :

$$v = \frac{C_3 \bar{R}}{R} \ln \left( \frac{R}{\bar{R}} \right) \quad (20)$$

where  $C_3$  is a constant. Hunderi and Ryum (1980) have recently commented that this solution of the Feltham analysis is only the first term in a series expansion. The corresponding distribution function for the full solution is not log-normal. The full solution shows a cut-off for high  $R$  rather than falling off to infinity as a log-normal distribution does. It therefore corresponds more closely with experimental findings than a log-normal distribution.

Feltham obtained,

$$\frac{dR^2}{dt} = C_4 \ln \left( \frac{R}{\bar{R}} \right) \quad (21)$$

where  $C_4$  is a constant. Setting  $R = R_{\max} = 2.5\bar{R}$  (using the time-invariant property of the log-normal distribution), and relying on the slowly varying nature of  $\ln(R/\bar{R})$  he obtained parabolic grain growth kinetics identical to (4).

Although Feltham did give consideration to grain size (and shape) distributions, the parabolic kinetics essentially arise from identical arguments to those which Burke and Turnbull used (see earlier). Using the Burke and Turnbull assumptions, it appears that any slowly varying distribution function can be used and will give parabolic kinetics.

#### 4.2 Louat's Theory Concentrating on the Diffusion Term

Louat (1974) argued that boundary motion is a random process (i.e. can be seen as sections of the boundary undergoing random walks) and that it is the diffusion term, and not the drift velocity term, which is important. It must be emphasised again that the physical basis for considering the diffusion term alone in (17) is not clear. He therefore set,

$$\frac{\partial f}{\partial t} = D \frac{\partial^2 f}{\partial R^2} \quad (22)$$

from (17), assuming D is independent of R, and solved (22) with the boundary conditions  $f(0,t) = 0$  and  $f(\infty,t) = 0$ . The solution he obtained was

$$f = \frac{C_6 x \exp(-x^2/4At)}{At^{3/2}} \quad (23)$$

where  $C_6$  is a constant and A a time-dependent parameter. If A is constant, on integrating (23) with respect to x, the total population  $N(t)$  is obtained:

$$N(t) = C_7 t^{-\frac{1}{2}}$$

where  $C_7$  is a constant. Louat asserted that this corresponds with a parabolic grain growth law as his analysis deals with linear dimensions and therefore, (he argues),  $N(t)$  represents, for instance, the inverse of the mean grain intercept (equivalent to a diameter). Louat ascribed grain growth kinetics with the exponent  $n > 2$  as due to time dependence of the parameter 'A' (equivalent to a diffusion coefficient).

The analyses of Burke and Turnbull (1952), Feltham (1957) and Hillert (1965) all specify grain radius R as representing grain size. A measure of R can be obtained from a 2-D section by either the line intercept method (specified in section 2.2), or by the area method in which the total area containing a number of grains is divided by that number (e.g. see Underwood (1970)). Burke and Turnbull, Feltham, and Hillert, assume that a 3-D parameter can be directly deduced from the measurement on a 2-D section through an isotropic material. This assumption will be discussed later in Section 6 on the Rhines and Craig (1974) theory.

The mean field theories of Feltham, Hillert and Louat are essentially statistical. The array of grains is represented by a distribution function  $f(R,t)$ , and the alteration in  $\bar{R}$  with time pursued by analytical means placing a spherical grain in an averaged environment. The shape distribution ( $f(n,t)$  in 2-D where  $n$  is the number of sides) is assumed time invariant (if mentioned at all). Topological considerations are not taken into account.

An important question which arises from these theories is "What fundamental property of (16) and (17), i.e.

$$j = -D \frac{\partial f}{\partial R} + fv$$

and

$$\frac{\partial f}{\partial t} = \frac{\partial}{\partial R} \left( D \frac{\partial f}{\partial R} \right) - \frac{\partial}{\partial R} (fv)$$

causes the Feltham, Hillert and Louat analyses, with varying assumptions, all to give a grain growth exponent of 2?"

##### 5. GRAIN GROWTH AS DISLOCATION CLIMB

Hillert (1965) presented an alternative method of attack on the grain growth problem to his statistical analysis described above. In this alternative method, he took an ideal 2-D array of hexagonal grains, with no tendency to grain growth, and introduced an imperfection i.e. a grain with 5 sides. This had to be balanced by a 7-sided cell (to preserve  $\langle n \rangle = 6$ ) and created a 5-7 pair (see Fig. 3 as discussed earlier). When the 5-sided grain eventually disappears, one of its neighbours in turn becomes 5-sided and the process is repeated. The "5-7 defect" is thus permanent and moves stepwise through the array of grains. For each step it takes, the number of grains is decreased by one. Hillert argued that the rate of grain growth is due to the combination of the number of defects per grain and the time a defect will need to make a grain shrink from the average size to zero. He then deduced parabolic grain growth kinetics. Cahn and Padawer (1965)

identified the movement of Hillert's 5-7 defects in the cell structure as equivalent to dislocation climb.

Morral and Ashby (1974) described a 3-D version of Hillert's 2-D model. They considered an assembly of fourteen-sided polyhedra in near equilibrium and then introduced thirteen or fifteen-sided grains, and other more serious "grain defects". A network of lines, which represented the grain structure, was constructed by joining the centres of all neighbouring grains through their common boundaries. These lines form a lattice ("lattice graph") with dislocations wherever there is a grain defect. Dislocation climb then corresponds to grain growth and involves three topological transformations:- cell annihilation, face annihilation and neighbour-switching. Morral and Ashby simply extended Hillert's 2-D analysis to 3-D to obtain the parabolic growth law, provided the defect density is constant. If the density decreases during grain growth, the exponent  $n$  is expected to become greater than 2.

Although this view of grain growth as the climb of "cellular dislocations" makes contact with topological considerations of grain growth, the analysis by Hillert (1965) to obtain parabolic kinetics is still essentially a mean field one.

#### 6. THE RHINES AND CRAIG TOPOLOGICAL ANALYSIS OF GRAIN GROWTH

In Hillert's (1965) 5-7 defect pair approach, the area of a shrinking 5-sided grain is shared with its neighbouring grains and its topological parameters change as topological transformations, such as neighbour-switching, occur. The parameters of the grains around it then also change. Thus, not only is its area shared out, but also its topological attributes. Hillert did not look beyond the shell of first neighbours around the shrinking grain. However, the changes in their shape and size must inevitably affect the second shell and beyond.

Rhines and Craig (1974) argued, in a paper which has become another of the classics in grain growth literature, that the volume (in 3-D) of the shrinking grain must be shared with grains throughout the whole system. Similarly, changes in topological parameters, the numbers of



edges, faces and vertices of grains, must also be propagated to every grain. The larger grains gain proportionately more of the volume to be shared out than the smaller grains. This is necessary if the grain-size distribution function is to remain time-invariant. Rhines and Craig introduced two new concepts, the sweep constant and the structural gradient.

### 6.1 The Sweep Constant

Grain boundaries throughout the system must migrate for these propagation processes to occur. Rhines and Craig described this as "grain boundary sweeping" and defined a "sweep constant,  $\theta$ " as the number of grains lost when grain boundaries throughout the whole structure sweep through the equivalent of unit volume of material. This definition was modified by Doherty (1975) to  $\theta^*$ , the number of grains which vanish when boundaries sweep through a volume equal to that of the mean grain volume  $\bar{V}$ . Rhines and Craig (1975) replied to Doherty's criticisms of their definition but no convincing arguments were offered either way. Hunderi (1979), however offered evidence that  $\theta^*$  was constant, but not  $\theta$ . Hunderi calculated  $\theta^* \sim 1.76$  on Hillert's (1965) mean field model of grain growth. Hunderi also found  $\theta^*$  constant and  $\sim 1.67$  using a 2-D computer simulation, which will be described in more detail in Section 10.2. The simulation, in contrast with mean field theories, accounts for local variations in particle environment. Hunderi's analysis of the Hillert model showed that  $\theta$  depends on  $\bar{R}$  and therefore varies during normal grain growth. This work by Hunderi does not conclusively prove that  $\theta^*$  is a constant for real granular materials and  $\theta$  not, as this could only be achieved by experiment. However, the balance of evidence is in favour of constant  $\theta^*$ . It would be difficult to find  $\theta$  or  $\theta^*$  directly by experiment.

### 6.2 Structural Gradient

The second concept introduced by Rhines and Craig was that of "structural gradient". Experimentally they found the product of the surface area per unit volume,  $S_V$ , and the surface curvature per grain,  $(M_V/N_V)$ , to be approximately a constant  $\sigma$  (see Fig. 8) i.e.

$$\frac{M_v S_v}{N_v} = \sigma \quad (24)$$

where  $M_v$  is the curvature per unit volume:

$$M_v = \int_{S_v} \left( \frac{1}{r_1} + \frac{1}{r_2} \right) dS_v \quad (25)$$

and  $N_v$  the number of grains per unit volume.  $r_1$  and  $r_2$  are the principal radii of curvature.

Rhines and Craig asserted that constant  $\sigma$  is a necessary consequence of the condition that the distribution of grain shapes ( $f(f,t)$  in 3-D where  $f$  is the number of grain faces) remains constant during grain growth although no proof of this is given.  $\sigma$  is a measure of the "structural gradient" in the system i.e. the tendency to grain growth. If the grains were all tetrakaidecahedra, with nearly flat faces,  $M_v$ , the surface curvature, would be very small and  $\sigma$  close to zero. As the distribution of grain shapes broadens,  $\sigma$  increases.

Doherty (1975) made the valid criticism that it is difficult to see the physical significance of  $(M_v S_v / N_v)$ , the product of the mean curvature per grain with the mean boundary area per unit volume. He suggested,

$$\alpha = \frac{M_v}{N_v} \quad (26)$$

where  $\alpha$  is the mean curvature per grain, as a useful alternative "structural gradient" representing the tendency to grain growth in the system. Experimentally,  $\alpha$  does not appear to be a constant (checked by Doherty using values taken from graphs in Rhines and Craig (1974)).

### 6.3 Analysis for Grain Growth Kinetics

The Rhines and Craig (1974) analysis of grain growth kinetics proceeds as follows, with modification by Doherty (1975) to use the sweep constant  $\theta^*$  rather than  $\theta$ . The mean pressure  $P$  on the boundaries is

$$P = \gamma \frac{M_v}{S_v} \quad (27)$$

and the mean boundary velocity

$$v = \frac{\mu \gamma M_v}{S_v} \quad (28)$$

The swept volume per second (per unit volume of specimen) is then  $vS_v$ ; so if  $\theta^*$  grains are lost, per unit volume, for each  $\bar{V}$ , then the rate of loss of grains will be

$$\begin{aligned} \frac{dN_v}{dt} &= \frac{\theta^* v S_v}{\bar{V}} \\ &= \theta^* \mu \gamma M_v N_v \end{aligned} \quad (29)$$

since

$$N_v = \frac{1}{\bar{V}} \quad (30)$$

For each grain lost, per unit volume, there is a net increase in volume of  $\bar{V}$  which is distributed, on average, over all the remaining  $N_v$  grains. Then, using (29) and (30),

$$\frac{d\bar{V}}{dt} = \left( \frac{dN_v}{dt} \right) \frac{\bar{V}}{N_v}$$

and

$$\frac{d\bar{V}}{dt} = \frac{\theta^* \mu \gamma M_v}{N_v} \quad (31)$$

If, and only if,  $\theta^*$ ,  $\mu$ ,  $\gamma$  and  $(M_v/N_v = \alpha)$  are constant and independent of time, (31) can be integrated to give a linear dependence of  $\bar{V}$  on time:

$$\bar{V} = \frac{\theta^* \mu \delta M_v}{N_v} t + \bar{V}_0 \quad (32)$$

where  $\bar{V}_0$  is the mean grain volume at time  $t = 0$ .

Rhines and Craig (1974) obtained such a linear time dependence for  $\bar{V}$  (measured as  $1/N_v$ ) experimentally for grain growth in high purity aluminium at 635°C (see Fig. 9).  $N_v$  was found by serial sectioning. Rhines and Craig drew attention to the important fact that with  $\bar{V}$  dependent linearly on  $t$ , the mean grain radius was growing as  $t^{1/3}$  (i.e.  $n$ , the growth exponent, equal to 3). Most other investigations have used (see e.g. Table 2), as mentioned earlier in Section 4.2, mean boundary intercept measurements on 2-D sections rather than finding 3-D parameters directly by serial sectioning, and values ranging from 2 to 4 for the exponent  $n$  have been found. Serial sectioning is very time consuming in comparison with mean grain intercept on a 2-D section.

#### 6.4 Comparison of Mean Grain Intercept and $(\bar{V})^{1/3}$ Methods

Therefore, an important question is whether a 3-D grain size can be deduced from mean grain intercept measurements on 2-D sections.

Rhines and Craig pointed out that the mean grain intercept is sensitive to the shape of the grains and will alter significantly if the grains are distorted e.g. by rolling. However, the mean grain volume  $\bar{V}$  will not change if the grains are rolled. Rhines and Craig stated "Neither mean grain intercept nor any other measurement that can be made upon a 2-D section through a material can be used to determine mean grain volume.  $N_v$  must be measured in 3-D space (i.e. by serial sectioning)". Measuring conventional mean grain intercepts on 2-D sections of the same specimens which they had examined by serial sectioning, they found that the mean grain intercept was proportional to  $t^{0.43}$  i.e.  $n = 2.3$ . This is in contrast with their  $t^{1/3}$  dependence for mean radius found from serial sectioning measurements of  $N_v (= 1/\bar{V})$ .

Cahn (1974), in a succinct review of grain growth theories, and Doherty (1984), have emphasised the importance, and to some extent

paradoxical nature, of these results. However, in the author's view Rhines and Craigs' statement above must be questioned. The validity of the statement depends on the anisotropy in the structure. For an isotropic structure, the mean intercept on a 2-D section will approximate to the 3-D mean grain radius. For an anisotropic one there will be a discrepancy. This suggests Rhines and Craig's recrystallised aluminium may have contained some residual anisotropy from the deformation process. It is this point i.e. that deductions about 3-D parameters cannot be made unless the degree of anisotropy in grain shape has been determined, that has implications for all experimental determinations of the grain growth exponent. Rhines and Craig were moving towards anisotropy as an explanation for their results (see Section 6.6) but did not express this explicitly.

#### 6.5 Analysis of Grain Growth Kinetics Continued

Returning to the question of how Rhines and Craig could have found a linear dependence of  $\bar{V}$  on time (equation (32)) if the structural gradient (defined as  $M_V/N_V$ ) in equation (31) is varying, Doherty (1975) suggested that the analysis could be repeated using equation (7) for  $v$ , rather than  $v = \mu P$ . The dependence of  $\bar{V}$  on  $t$  would then be linear if

$(\frac{M_V}{N_V})(1 - \frac{P_0}{\gamma} \frac{S_V}{M_V})$  were constant. Substituting values from Rhines and Craig (1974) for  $M_V S_V$  and  $N_V$ , this can only be achieved if  $P_0/\gamma \sim 0.1 \text{ cm}^{-1}$ . Grey and Higgins (1972, 1973) reported values in this region for grain boundary migration in lead and therefore Doherty (1975) concluded that this is a possible explanation.

#### 6.6 Steady State Conditions

It should be noted that Rhines and Patterson (1982) found the linear increase in mean grain volume,  $\bar{V}$ , with time does not occur in the initial period immediately after recrystallization begins. During this period, the sweep constant  $\theta^*$  and the structural gradient  $\alpha$  (or  $\sigma$ ) are not constant and steady state grain growth conditions are not established. Rhines and Patterson (1982) showed that the rate of grain growth is strongly affected by prior strain. Small prior strains give

wider size distributions and faster grain growth. The wider size distribution is equivalent to a higher structural gradient.

Rhines and Craig (1974) found that a steady state appears to be established for topological parameters (i.e. they tend towards constant values) much sooner than for grain shapes. They suggest that the mean intercept dependence on  $t^{0.43}$ , in contrast with mean radius dependence on  $t^{1/3}$  (from serial sectioning), might be due to a relative area decrease resulting from a continued approach to equiaxedness (and shape steady state) after topological parameters have reached steady state. Rhines and Craig did not examine whether mean grain intercept tended to become equal to mean grain radius with continued annealing time. This ties in with the discussion of the relationship between mean grain intercept and mean radius in Section 6.4 and the role of residual anisotropy. The structural gradient is a shape dependent parameter (at least on Doherty's (1975) definition of  $\alpha = M_v/N_v$ ) and as such will vary during the approach to shape steady-state, after topological steady-state has been established. The variation in  $\sigma$ , the structural gradient defined by Rhines and Craig (1974) as  $(M_v S_v / N_v)$  cannot be large during this regime, or else  $\bar{V}$  would not be linearly dependent on  $t$  experimentally.

#### 6.7 Summary and Discussion of the Rhines and Craig Analysis:

In summary, Rhines and Craig (1974) arrived at a linear dependence of  $\bar{V}$  on time, employing two supposed constants,  $\theta^*$  the sweep constant (defined in modified form by Doherty (1975) as the number of grains lost when grain boundaries sweep through a volume equal to the mean grain volume  $\bar{V}$ ) and the structural gradient  $\sigma = M_v S_v / N_v$  (alternative proposed by Doherty (1975)  $\alpha = M_v / N_v$ ). Rhines and Craig confirmed the linear time dependence of  $\bar{V}$  experimentally and commented on the contrast between the dependence of mean grain radius on  $t^{1/3}$  and of 2-D mean grain intercept on  $t^{0.43}$  for their specimens. This discrepancy is probably due to grain shape anisotropy. With further annealing, mean grain intercept should tend to become equal to mean grain radius, but with, according to Rhines and Craig, a  $t^{1/3}$  dependence.

In a system in which grain boundary migration is relatively slow (i.e. one well below its melting point, in contrast with the aluminium at 635°C used by Rhines and Craig) could  $\theta^*$  be constant? Migration could be so slow that the system is not in quasi-equilibrium constantly propagating volume and topological changes through the structure. The volume and topological changes would only be able to propagate locally. This scenario deserves further investigation. It echoes Hillert's dislocation climb model of grain growth (Section 5) in which only nearest neighbour cells change their topological parameters when a cell is annihilated. Aspects of the question of equilibrium are further discussed in Section 10.3.

The mean field theories predict that mean grain radius will be proportional to  $t^{1/2}$ . This brings us to the real core of the problem. Rhines and Craig find experimentally with serial sectioning mean grain radius is dependent on  $t^{1/3}$  and justify this algebraically. Why the discrepancy? The central question here is:-

"How has the Rhines and Craig analysis departed from the basic mean field approach?"

The answer appears to lie, for all the debate about their definitions, in the introduction of the sweep constant and the structural gradient. However, it is not clear whether the Rhines and Craig analysis is still mean field in type, in that the sweep constant and the structural gradient are still averaged through the whole ensemble then allowed to act on an individual grain. The departure from the Burke and Turnbull analysis occurs with equation (29) and the introduction of  $\theta^*$ . The sweep constant represents grain boundary movement throughout the structure in response not only to volume sharing as grains shrink, but also to topological requirements. Propagation of topological changes through structures is thus taken into account, in contrast with the basic mean field theories.

However, the Rhines and Craig  $t^{1/3}$  dependence for  $(\bar{V})^{1/3}$  has not

been confirmed or otherwise by other experimenters and it is difficult to gauge how far the 2-D sectioning results give values of  $n$  not equal to 3 because of grain shape anisotropy.

## 7. TOPOLOGICAL CHARACTERISTICS OF THE STEADY STATE

Rhines and Craig (1974) examined the topological paths of transformation which could be taken by grains in polycrystalline aggregates but did not focus on the distribution of the topological parameters and the fundamental causes for these distributions. This Blanc and Mocellin (1979) and Carnal and Mocellin (1981) set out to do.

### 7.1 Monte-Carlo Simulations to Obtain Distributions of Topological Parameters

Aboav (1970) found in highly dense, sintered MgO that a correlation existed between the number of sides of a grain,  $n$ , and the average number of sides,  $m_n$ , of its neighbours:

$$m_n = 5 + \frac{8}{n} \quad (33)$$

Weaire (1974) explained Aboav's correlation simply on the basis of Euler's theorem and suggested a more general equation:

$$m_n = 5 + \frac{6 + \mu_2}{n} \quad (34)$$

with

$$\mu_2 = \sum_1^{\infty} (n - 6)^2 f_n \quad (35)$$

$f_n$  is the fraction of grains with  $n$  sides and  $\mu_2$  the variance in the number of sides. This relationship (34) will be discussed again in Section 9.3.

Morral and Ashby (1974), as mentioned in Section 5, suggested elementary topological transformations for microstructural evolution:



(1) Disappearance (termed event A) and appearance (termed event B) (in 2-D) of 3-sided grains.

(2) Neighbour-switching (termed event C).

Blanc and Mocellin (1979) dealt with 2-D sections through statistically isotropic microstructures. They used a Monte-Carlo simulation of the coordination changes in a population of grains when the elementary topological transformations A, B and C repeatedly occur and predicted the distributions  $f_n$  and  $m_n$  tending to be established in the steady-state. These agreed reasonably well with their experimental data. Their predicted  $f_n$  distribution could be fitted to a log-normal distribution, but they state,

"Curve fitting may always be practised but an apparently very good numerical agreement with experiment should not be mistaken for proof that no other functional relationships could provide similar good fits."

They also comment that there is strong evidence for grain to grain correlations,

"It would be remarkable if the rigorous solution were log-normal."

This remark is relevant to a subsequent discussion (Section 8) of the role of the log-normal distribution by Kurtz and Carpay (1980a).

## 7.2 Analytical Method to Obtain $f_n$

Carnal and Mocellin (1981) obtained the distribution of grain coordination numbers in plane sections of polycrystals by an analytical technique rather than by the Monte-Carlo simulation used by Blanc and Mocellin (1979). In the analytical approach, the elementary topological transformations A, B and C occur repeatedly at random, thus transferring grains from one "shape class-n" to another. This "collective behaviour" of the whole grain population is then treated by statistical arguments and Carnal and Mocellin (1981) show, for  $n \geq 3$

$$\begin{aligned}
& [1 - f_3 - f_4 - \dots - f_{n-1} - 3P(r = n)][P(A) - P(B)] \\
& = 2P(C) [P(i = n) - P(k = n - 1)] \qquad (36)
\end{aligned}$$

where  $f_n$  is the fraction of grains with  $n$  sides,  $r$  is the initial number of sides of any one of the neighbours of an  $n$ -sided grain,  $P(r = n)$  is the probability that  $r = n$ ,  $P(A)$  is the probability of a 3-sided grain disappearing,  $P(B)$  the probability of a 3-sided grain appearing,  $P(C)$  the probability of a neighbour-switching event,  $i$  is the number of sides of any grain neighbouring the  $n$ -sided grain prior to a neighbour-switching event and  $k$  the number of sides after.

The above equation must be satisfied if topological stability is to be maintained in a random plane section of a polycrystal. It is not possible to obtain the  $f_n$  distribution unless more information is available about the three probability distributions  $P(i = n)$ ,  $P(k = n)$ , and  $P(r = n)$ . These describe the interactions between grains and their nearest neighbours and as such invoke some physics (in contrast with the purely statistical arguments used to determine the collective behaviour of the grains up to this point). These probability distributions may assume different behaviours in different materials and environments.

Equation (36) also describes the existence of a balance between the elementary topological transformations A, B, and C. Carnal and Mocellin (1981) have commented on various possibilities for  $P(A)$ ,  $P(B)$  and  $P(C)$ . If "normal" grain growth is defined as that process which takes place in a topologically stable polycrystal, then a fixed ratio must be maintained between the net number of grains disappearing from the polycrystal and the number of other grains which take part in neighbour-switching. Control of grain growth kinetics may therefore be effected through either or both of the elementary transformations cell appearance/disappearance or neighbour-switching (A + s, or C) not necessarily through just the disappearance of 3-sided grains (in 2-D). Carnal and Mocellin (1981) predicted that there would be an average of 4 neighbour-switching events for every 3-sided grain disappearance.

It is not clear, in these two models (Blanc and Mocellin (1979) and Carnal and Mocellin (1981)), whether a polycrystalline grain boundary

network is initially fed into either the computer simulation or the analytical method. If it is, both models have strong links with the 2-D computer simulations of soap froths (to be discussed later in Section 11.2) in which the elementary topological transformations are allowed to occur, given certain constraints, in a 2-D network, and the time evolution of the network then examined. Blanc and Mocellin and Carnal and Mocellin have, however, waited for a steady-state to be achieved in the topological properties and then examined the distributions of topological parameters, regardless of the time evolution.

## 8. KURTZ AND CARPAY STATISTICAL THEORY OF NORMAL GRAIN GROWTH

### 8.1 Analysis

Kurtz and Carpay (1980a) constructed a detailed statistical theory of grain growth, placing emphasis on the supposed log-normal distribution of grain sizes and shapes asserted, for instance, by Feltham (1957). The prime new feature of the Kurtz and Carpay (1980a) theory is their division of the grains into topological classes, each with a log-normal distribution of grain sizes. This is in contrast with those statistical theories which are based on a single geometrical shape which fills space and is then allowed to have statistically distributed sizes (implicit in e.g. the early mean field theories). In this theory, both sizes and shapes are allowed to vary whilst the requirement for space filling is retained. However, this does make it much more difficult to rigorously specify the transformation from 2-D to 3-D (i.e.  $n \rightarrow f$  and, in Kurtz and Carpay's terms,  $D_s \rightarrow D_v$  where  $D_s$  is the equivalent planar diameter ( $D_s \equiv s/\pi$  where  $s$  is the perimeter of the grain) and  $D_v$  is the equivalent spherical diameter ( $D_v \equiv (6V/\pi)^{1/3}$  where  $V$  is the volume)).

Growth is controlled by the rate of loss of grains from the lowest topological class, as discussed by Rhines and Craig (1974). Kurtz and Carpay solved for the grain growth kinetics in each class as well as transfer rates between classes. When a grain transfers between classes it loses (or gains) one face, two corners and three edges, i.e. a

3-sided face. Kurtz and Carpay made a number of simplifying assumptions in order to solve the equations.

- (1) log-normal distribution of sizes and shapes and of sizes within each topological class.
- (2) time-invariance of distributions.
- (3) growth controlled by rate of loss of grains from lowest topological class accompanied by discontinuous transfer of growing grain to next topological class.

$$(4) \quad \frac{D_v}{2M_v} = \ln \left( \frac{F}{F_{med}} \right) \quad (3-D) \quad (37)$$

where  $M_v$  is the mean curvature per unit volume ( $\rho$  in 2-D),  $F$  the number of faces and  $F_{med}$  the median number of faces.

$$\frac{D_s}{2\rho} = \ln \left( \frac{n}{n_{med}} \right) \quad (2-D) \quad (38)$$

- (7) 2-D microstructural evolution reflects the essential features of that in 3-D.

The origin of equations (37) and (38) is not clear and neither is Kurtz and Carpay's reason for considering median values rather than means.

Kurtz and Carpay note that "The key problem is to find the correct functional relationship in 3-D between the three basic parameters,  $F$ ,  $D_v$  and  $M_v$ . However, a theory based solely on  $D_v$ ,  $F$  and  $M_v$  would be of limited value because of the labour and effort required for serial sectioning". Therefore, they aim to produce a theory based on the 2-D planar section parameters which can then be transformed to 3-D. This is a constructive attitude towards the problem connected with using 2-D parameters raised by Rhines and Craig (1974).

Using their calculated rates of transfer between classes, Kurtz and Carpay were able to explain how the median diameter of those classes in which grains are shrinking still manages to increase in such a way as to keep their number a constant fraction of the total population (see Fig. 10). In the successive "hand-me down" transfer between classes, grains enter a class with slightly larger diameters than the median of the class they are entering. Hence the median diameter can increase even though individually all the grains in that class are shrinking. Transfer rates increase the lower the topological class, thus keeping pace with the required changes in median.

In their analysis, Kurtz and Carpay (1980a) found a parabolic growth law for the median grain size of the whole population as well as for the median grain size in each topological class. They also showed that the Rhines and Craig (1974) structural gradient ( $M_v S_v / N_v$ ) was a constant under their theory, related to the variance in the distribution of faces  $\sigma^2(F)$  and the variance in the distribution of sizes  $\sigma^2(D)$ . (Note  $\sigma$  denotes standard deviation not structural gradient here.) Once normal grain growth is established, the growth rate is a strong function of  $M_v S_v / N_v$  where

$$\left( \frac{M_v S_v}{N_v} \right)^2 = \sigma^2(D) + \sigma^2(F) \quad (40)$$

The dependence on  $\sigma^2(D)$  has been confirmed by Rhines and Patterson (1981) and was briefly discussed earlier in Section 6.6.

Kurtz and Carpay also conclude that stability in normal grain growth arises from a maximum, at any instant in time, in the average grain boundary velocity as a function of increasing grain size. They predict,

$$D_{\max} = e D_{\text{med}} \quad (41)$$

where  $e$  is the exponential  $e \approx 2.718$ .

The log-normal distribution, Kurtz and Carpay argue, is a fundamental characteristic of grain growth and of other phenomena such

as the size distribution in crushed powders and in ultrafine evaporated metal powders. They suggest that for grain growth it arises because when a four-faced (in 3-D) grain vanishes, the four adjacent grains increase in diameter by an amount proportional to their diameter. Kurtz and Carpay then show how the diameters can approach a log-normal distribution. However, it is not clear their argument is valid. In Fig. 11 it would appear that when a 3-sided grain disappears in 2-D the adjacent grains increase in diameter in inverse proportion to their diameter. The general applicability of the log normal distribution to grain growth is not universally accepted (see for instance Blanc and Mocellin's comment at the end of Section 7.1).

Kurtz and Carpay go on to test their theory against experiment (1980b) and to compare Hillert's predicted grain size distribution with their own, which, they conclude, fits the data better.

## 8.2 Experimental Results

The Kurtz and Carpay (1980b) experimental results in grain growth in Ni-Zn ferrites confirmed the following conclusions from their statistical theory.

- (1) The grains can be divided into topological classes with markedly different growth rates.
- (2) The median diameter of the overall distribution and of the distributions in the individual topological classes grow parabolically, both on 2-D sections and in 3-D (as measured by serial sectioning).
- (3) Growth constants agree to within 10% of those predicted, except for the lowest topological class.
- (4) Planar measurements can be used to make deductions about 3-D parameters (confirmed by serial sectioning).
- (5)  $D_{\max} = eD_{\text{med}}$ .

(6) Time-invariance of standard deviations of log (size) and log (shape) distributions.

(7) Constant structural gradient ( $M_v S_v / N_v$ ).

The Kurtz and Carpay (1980a, 1980b) statistical theory is wide-ranging and detailed. It is surprising that nowhere do they specifically tackle the difference between the Rhines and Craig dependence of mean grain radius on  $t^{1/3}$  and their own  $t^{1/2}$  law. Kurtz and Carpay's only comment in this direction is that  $t^{1/3}$  laws have often been found when the initial grain size ( $\bar{R}_0$  in equation (5)) is neglected, or if the growth law exponent is extracted from a log D-log t plot, which can give misleading results. Neither of these criticisms can be levelled at Rhines and Craig. It is worth noting that very low levels of impurities can affect boundary migration and Rhines and Craig (who used 99.99+% Al in their experiments) did not present any microanalysis of grain boundaries to prove that they were clean enough for their migration not to be impeded by foreign atoms. However, without any evidence either way, it is not possible to pursue further this line of discussion about the discrepancy.

## 9. STRUCTURE OF RANDOM CELLULAR NETWORKS

Before moving on to look at the recent computer simulations of grain growth, it is pertinent to examine the latest thoughts on the structure of random cellular networks which can give insight into grain growth.

### 9.1 Lewis' Law

Lewis' Law (Lewis (1928)) for a 2-D cellular network states that the average area of an n-sided cell,  $\bar{A}_n$ , is linearly dependent on n:

$$\bar{A}_n = B(n - n_0) \quad (42)$$

with

$$\beta = \left(\frac{A_0}{F}\right)\lambda \quad (43)$$

and

$$n_0 = 6 - \frac{1}{\lambda} \quad (44)$$

Here  $A_0$  is the total area available to F cells and  $\lambda$  is a Lagrange multiplier which, prior to Rivier (1983), was apparently undetermined. Rivier (1983) identified  $\lambda$  as a parameter representing the ageing of the structure.

Lewis' Law is a mathematical law which should hold for any space-filling structure as long as it is in statistical equilibrium. It is a consequence of the balance between entropy and organized form (space-filling). This will be discussed in further detail in Section 9.4. Suffice to say that, if a mosaic does not obey Lewis' law, then the average area of its constituent cells is not regulated purely by the space-filling requirement but by a specific physical (for metallurgical aggregates) or biological law (Rivier and Lissowski (1982)). Lewis' Law is obeyed by mathematical mosaics formed by the Voronoi construction applied to a random array of centres (Crain (1979)). In the Voronoi construction, each of the centres is assigned a cell containing all points nearest to it (see Fig. 12) e.g. by drawing the perpendicular bisecting planes (in 3-D) or lines (in 2-D) to the lines joining any two centres.

Rivier (1983) showed that by time-differentiating Lewis' law (42) von Neumann's law (1952), first mentioned in Section 3 could be directly obtained:

$$\frac{d\bar{A}_n}{dt} = \gamma(n - 6) \quad (45)$$

Here it is simply a mathematical consequence of space-filling rather than the result of surface tension requirements in a 2-D soap froth as originally argued by von Neumann.  $\gamma$  is (according to Rivier (1983)) a constant and proportional to the surface tension of the liquid forming



the froth.  $\lambda$ , the Lagrange multiplier, in (43) and (44) is therefore related to surface tension. This indicates though, in the author's understanding, that a physical force is acting and therefore that von Neumann's Law is not purely a space-filling requirement. This leaves an unresolved difficulty. Do soap froths (and other structures) obey (45)? If so how can this be reconciled with the fact that they do not obey (42)? Lewis' (42) and von Neumann's (45) laws can be generalized to 3-D (Rivier (1983)) and hold irrespective of the probability distribution  $\{p_n\}$  for the number of cells with  $n$ -sides, provided the system is in statistical equilibrium i.e. maximum entropy subject to constraints (see Section 9.4).

Rivier (1983) has not checked his 3-D versions of von Neumann's and Lewis' laws with experiment. He assumes that the derived relationships do apply to soap froths, along with "ideal" structures based on, for instance, the Voronoi construction. This point will be returned to in Section 9.4.

## 9.2 Asymptotic Evolution of 2-D Soap Froth

Weaire and Kermode (1983a) asked

"What form does the evolution of the structure of a 2-D soap froth take in the limit  $t \rightarrow \infty$ ?"

Smith (1952) suggested, as referred to earlier.

- (1) A fixed distribution of sizes and shapes.
- (2)  $\bar{A}$  proportional to  $t$ .

Weaire and Kermode commented that there is no rigorous theoretical basis for such propositions although if (1) is assumed, (2) follows by a simple dimensional argument (as in Burke and Turnbull (1952)). For 2-D, from Smith (1952) and Kikuchi (1956),  $\mu_2$ , the variance in  $f_n$ , (equation (35)), is approximately 1.5 for the limiting distribution.

Weaire and Kermode drew attention to the work of Aboav (1980) who had reanalysed Smith's photographs of 2-D soap froths but with many more cells, to find how the average linear intercept  $D$  changed with time. He found, in contrast with (1) and (2):

(3)  $\mu_2$  proportional to  $t$  up to  $\mu_2 \sim 3$  and possibly beyond.

(4)  $D$  proportional to  $t$ .

The discrepancy between (2) and (4) may be due to surface effects affecting the small samples of bubbles examined by Smith. (All experimental 2-D froths were made by forming a thin layer of bubbles between two glass plates.) However, Weaire and Kermode briefly indicate that the whole question of the long-term evolution of 2-D soap froths is laid open to question. They suggest that the ultimate structure may be "fractal". Fractals were first named by Mandelbrot (1977). Weaire and Rivier (1984) show a possible fractal structure for a soap froth system (see Fig. 13). In the author's view, the stability of such a structure even in an ideal system is unlikely. Would not the large central grain tend to subsume the tiny ones around it? It would be useful to see some analysis of the possibility of such structures. In any case, Weaire and Kermode (1983b, 1984) are pursuing the 2-D evolution of soap froths by computer simulation to find, if possible, some insight into the long term behaviour. These computer simulations will be described in Section 10.3. If soap froths do tend to fractal structures, or even if merely  $\mu_2$  continues to be proportional to  $t$  even for high  $\mu_2$ , the point must be made that this is not "normal" grain growth and the question raised as to whether soap froth behaviour can be legitimately used for 2-D networks to model growth in polycrystals. If not, what is the reason for the divergence? The questions will be discussed in Section 10.3.

### 9.3 The Aboav-Weaire Law

The Aboav-Weaire law for 2-D networks has been mentioned previously in Section 7.1 on "Topological Characteristics of the Steady-State". Aboav (1970) found equation (33) empirically for ceramics, giving the correlation between the number  $n$  of sides of grain and the average number  $m_n$  of sides in its neighbours. Weaire (1974) gave the more

general equation (34). To be precise, Aboav found

$$m_n = 6 - a + \frac{6a + \mu_2}{n} \quad (46)$$

with  $a \sim 1.2$ .

Lambert and Weaire (1983) suggested that this empirical result shows that there exists a certain class of 2-D random networks whose nearest-cell correlation function,  $m_n$ , is linearly related to  $1/n$  and is characterized by a single parameter 'a' with 'a' related to  $\mu_2$ . They showed that under certain conditions, 'a' could be obtained from a knowledge of the distribution function  $f_n$ . They deduce that 'a' is related to the kurtosis of  $f_n$ . The 3-D version of the Aboav-Weaire law will be referred to in the next section (9.4).

#### 9.4 Maximum Entropy Considerations

Rivier (1985) set out to find, using the methods of statistical mechanics, the most probable distributions of cell sizes and shapes in random space-filling cellular structures such as foams, metallurgical grain aggregates and biological tissue. Kikuchi (1956) was the first to propose that statistical mechanics could be useful.

Rivier's approach is termed statistical crystallography. The basic proposition is that an assembly of an enormous number of atoms, cells, or metallurgical grains will take up one of the most probable configurations, subject to a few, unescapable mathematical constraints like space-filling (although it must be noted that this applies only to 100% dense materials). Specifically, the constraints are, for an "ideal" system (for 2-D), with  $p(n,A)$  the probability of finding an n-sided cell with area A.

$$\sum p(n,A)n = 6 \quad \text{Euler-topology} \quad (47)$$

$$\sum p(n,A)A = A_0/F \quad \text{space-filling} \quad (48)$$

$$\sum p(n,A)[A - \bar{A}_n] = 0 \quad \text{correlation} \quad (49)$$

Here  $A_0$  is the total area containing  $F$  cells and  $\bar{A}_n$  is the average area of an  $n$ -sided cell. In 3-D, the relation corresponding to (49) is much weaker, i.e. equation (13):

$$\langle f \rangle = 12 / (6 - \langle n \rangle)$$

The structure will be in statistical equilibrium if any topological rearrangement of the cells leaves the entropy invariant. The entropy  $S$ :

$$S = -\sum p(n,A) \ln[p(n,A)] \quad (50)$$

and the Maximum Entropy Formalism of Probability Theory states that the structure will take up the most probable distribution  $p(n,A)$  which maximises the entropy with the given constraints. An equation of state, analogous to an ideal gas law, giving a relationship between averaged measurable properties of the structure, can be obtained. Any deviation from the equation of state obtained using the minimal constraints given above, indicates that further constraints are operating.

Rivier (1984) first proved "structural microreversibility" i.e. the expected values of the statistical variables are unaffected by the elementary topological transformations of neighbour-switching, face appearance/disappearance, and cell appearance/disappearance. Hence, he deduced the Aboav-Weaire law (33) and its 3-D analogue:

$$n \bar{m}_n = 5f - 11 - C(f - 1 - n) \quad (51)$$

where  $C$  is a constant. Equation (51) is a new result which has not been checked experimentally.

Rivier (1985) then established that the equation of state for an "ideal" system, to which only the minimal constraints given above apply, was Lewis' law, equation (42):

$$\bar{A}_n = \beta(n - n_0)$$

Lewis' law, as commented earlier, therefore arises as a consequence of balance between entropy and organised form (space-filling).

Rivier then proceeded to obtain the most probable distribution of the statistical variables (the structural equivalent of the Boltzmann distribution). Polycrystals, however, do not obey Lewis' law (Aboav and Langdon (1969) (MgO), Beck (1954) (Al), Simpson et al (1967)(Pb)). They are "non-ideal" random structures. An additional constraint is necessary. This is an energy requirement:

$$\sum p(n,A,s)s = E/F \quad (2-D) \quad (52)$$

where  $p(n,A,s)$  is the probability of an  $n$ -sided grain with area  $A$  and perimeter  $s$ , and  $(E/F)$  is the average energy/grain. The other constraints (47), (48) and (49) are recast to give:

$$\sum p(n,A,s)n = 6 \quad (\text{topology}) \quad (53)$$

$$\sum p(n,A,s)A = A_0/F \quad (\text{space-filling}) \quad (54)$$

$$\sum p(n,A,S)[(1-\eta)A + \eta s - \bar{B}_n] = 0 \quad (\text{correlation}) \quad (55)$$

$\eta = 0$  if Lewis' Law applies (i.e.  $\bar{B}_n = \bar{A}_n$ ), but  $\eta = 1$  if a perimeter law applies and  $\bar{B}_n = \bar{R}_n$ . The analysis revolves around showing that, of these two alternatives,  $\eta = 1$  gives the higher entropy and hence the most probable distribution. (It is not clear why the energy constraint does not appear to be necessary for soap froths where Lewis' law seems to be taken to apply by Rivier (1983); see comments in Section 9.1.) The additional energy constraint gives rise to a different equation of state:

$$\bar{R}_n = \beta'(n - n_0') \quad (56)$$

where  $\bar{R}_n$  is the mean radius of  $n$ -sided grains. This relationship was

found by Aboav and Langdon (1969), Beck (1954) and Simpson et al (1967). It was also found in computer simulations by Srolovitz et al (1984) (described in Section 10.5).

The predicted size distribution of grain areas, with the new constraint, is exponential. The Srolovitz et al (1984) simulation, and experiments by Beck (1954) and by Aboav and Langdon (1969), all give results which agree with this distribution although Aboav and Langdon described their experimental results in terms of fit to a much more complicated distribution. The predicted size distribution is time-invariant when scaled by  $\bar{R}$ . In contrast, the predicted shape distribution, which depends on  $n$  and  $A$ , broadens with time. Rivier cites a number of experimental references in support of his derived shape distribution. However, of these none apply to metals. Two refer to ceramic systems, Lantuéjoul (1978) and Blanc and Mocellin (1979). However, examination of these papers shows no evidence to support a change in the shape distribution with time.

It would be interesting to find how far the experimental evidence does support Rivier's "non-ideal" system conclusions of:

- (1) time-invariant size distribution,
- (2) time varying shape distribution.

If there is agreement with these conclusions, new light is thrown on the "asymptotic" behaviour of soap froths, discussed in Section 9.2. For the question then arises as to whether the "scaling" attribute of normal grain growth applies only to the size distribution and not to the shape. Time invariance of the shape distribution has often been assumed (e.g. Feltham (1957)). Soap froths may then represent non-ideal systems to some extent and therefore be useful in modelling polycrystalline grain growth after all.

#### 9.5 Topological Properties of Trivalent Cellular Structures

The cells in metallurgical grain aggregates consist of trivalent polyhedra i.e. surface tension effects tend to eliminate vertices with

more than three faces meeting at the point. Fortes and Ferro (1985a) have examined the properties and types of individual trivalent polyhedra in detail, arguing that this is an important basis in studies of the 3-D packing of grains. In particular, they have concentrated on the enumeration of the distinct, non-isomorphic, (i.e. topologically inequivalent), polyhedra with  $F$  faces. They make no attempt however to indicate the significance of their results for 3-D packing.

In their second paper, Fortes and Ferro (1985b) make the point that there is excess free energy associated not only with faces but also with edges and vertices. Generally treatments of grain growth rely on the equation for the pressure difference across a curved interface (3) and ignore the contributions of edges and vertices. Fortes and Ferro give a neat vectorial representation of the forces acting on these elements and discuss the topological transformations which accompany grain growth in some detail. They identify restrictive topological rules for the neighbour-switching operation e.g. an edge in a triangular face cannot switch as a two-sided face would result. The role of vertices in grain growth will be returned to in Section 10.5.1.

Fortes and Ferro (1975b) state that the evolution of a 3-D structure can be completely determined if the mobilities of its edges, faces and vertices, and the dependence of the driving forces on face and triple line energy, are known. They also point out that little attention has been given to anisotropy in grain boundary (face) and triple line (edge) energy. However, they make no contribution as to how to treat a whole ensemble of such velocity/force equations, even assuming the mobilities, energies, and orientation dependencies of energies were known.

Fortes (1986) shows that for an infinite space-filling structure of trivalent polyhedra, the average number of faces  $\bar{F}$  in individual cells (grain boundaries in isolated grains) cannot be less than 8. For a finite structure, but with all topological elements saturated including the peripheral ones (to form what is called a hyperpolyhedron)  $\bar{F} \geq 4$ . In addition, there is no upper limit to  $\bar{F}$  in such structures (saturated or unsaturated). In metallurgical aggregates,  $\bar{F}$  is usually  $\sim 14$ . Values close to 8 have never been reported and could only possibly occur in highly anisotropic structures.

These papers are a useful adjunct to the mainstream development of grain growth theories but do not appear to make any significant contributions to the drive towards understanding the kinetics of grain growth.

## 10. COMPUTER SIMULATION OF GRAIN GROWTH

Computer simulations of grain growth can be divided into those which set up a system of equations for statistical quantities and those which simulate the evolution of a network directly. Novikov's Model (10.1) and the Linear Bubble Growth Model (10.2) fall into the former category. Soap froth simulations (10.3), Ceppi and Nasello's Model (10.4) and the Monte Carlo simulations of the Exxon Group (10.5 and 10.6) fall into the latter category. Anderson (1986) has recently reviewed computer simulation of grain growth.

### 10.1 Novikov's Model

Novikov (1978) was amongst the first to present a computer simulation of grain growth, prompted by the experimental findings that the grain growth exponent is always greater than 2, even for zone-refined high purity metals (see Table 2) where supposedly no pinning forces are effective (Simpson et al (1971)). Novikov proposed a new statistical approach based on absolute reaction rates supplemented by calculations of the contact probability of grains of different size and orientation. To carry out the computer simulation, Novikov assumed:-

- (1) Grains have random orientations.
- (2) Driving force for growth is decrease of total grain boundary energy only.

and aimed to find the size distribution (shape was not taken into account) after a period of grain growth, given:-

- (1) The number of grains at  $t = 0$ .
- (2) The initial size distribution.



(3) The value of  $\mu\gamma$  (mobility x grain boundary energy).

The size distribution was assumed to be log-normal. A grain can grow at the expense of some of its neighbours, although at the same time it may be consumed by other neighbours. This was taken into account by examining the change in the number of grains in each size-class successively. The simulation can therefore be used to find the alteration in  $\bar{D}$ , the mean grain diameter, with time. The grain growth exponent was found to be  $n = 2.2$ . The importance of not neglecting the initial grain size  $\bar{D}_0$  was emphasised. Novikov deduced values for  $\alpha$ :

$$\bar{D} \geq \alpha \bar{D}_0$$

if

$$\bar{D}^n = kT$$

is to be valid rather than

$$\bar{D}^n - \bar{D}_0^n = kT$$

Novikov stated that the rate of grain growth decreases with increase in the width of the initial log-normal size distribution (although his Fig. 4 suggests the opposite). This statement is contrary to the experimental results of Rhines and Patterson (1982) and the argument that the wider size distribution gives a higher structural gradient and hence greater tendency to grain growth.

Novikov's approach is essentially mean field. Each grain is surrounded by grains with a log normal distribution of sizes. The probability that a grain of one size contacts a grain of another size can be calculated. The statistical probability of a certain contact area between grains of different sizes can also be found. Novikov's approach can be extended to include the effects of pinning forces, and of texture (Novikov (1979)). Texture spread has a strong influence on grain growth kinetics. The acceleration of growth is especially appreciable when minor texture components strengthen.

## 10.2 Linear Bubble Growth Model

Hunderi et al. (1979a) pointed out that the theories of Feltham (1957), Hillert (1965) and Louat (1974) which treat grain growth as a continuous process in which the material in a disappearing grain is distributed over the whole system, do not allow for the fact that a grain of a particular size can grow in one environment (where it is surrounded by smaller grains) and shrink in another, i.e.  $R_{crit}$ , the critical radius, varies with position. They proposed a linear bubble growth model. In this model (see Fig. 14), the bubble  $i$  makes contact with a number of other bubbles from  $-j$  to  $+j$ , depending on the relative size of the grains. (The number of contacts is fewer the smaller  $i$  in size). The area over which material is exchanged between one particular grain and its neighbours depends on the surface area of the grain. Material is exchanged as the result of the pressure difference between bubbles of different sizes,  $R_i$  and  $R_j$ :

$$\frac{dR_i}{dt} = -\frac{M}{R_i^2} \sum_j^{+j} \max A_{ij} \left( \frac{1}{R_i} - \frac{1}{R_j} \right) \quad (57)$$

where  $A_{ij}$  is the area of contact between  $i$  and  $j$  (in the general case not known). The set of coupled equations is solved for a large number of grains to obtain the grain size distribution. This is more peaked than log-normal but has a cut-off at large grains which is more reasonable experimentally than a log-normal distribution. It is also more peaked than Hillert's distribution. Hunderi et al. point out that Hillert's model corresponds with

$$\frac{dR_i}{dt} = -M \left( \frac{1}{R_i} - \left\langle \sum_j \frac{A_{ij}}{R_i^2} \cdot \frac{1}{R_j} \right\rangle \right) \quad (58)$$

with each particle  $j$  corresponding to averaging over the whole size distribution. Hunderi et al.'s model gives the same growth kinetics as Hillert's though, with  $(\bar{R})^2$  linearly related to time. They go on to use their model:-

- (1) To examine the sweep constants  $\theta$  and  $\theta^*$  as discussed earlier (Hunderi (1979)).
- (2) To simulate stagnation in grain growth due to pinning by second phase particles (Hunderi and Ryum (1981)).

In Hunderi and Ryum (1981), normal grain growth is examined with a larger number of grains than in Hunderi et al. (1979), and over longer time scales. It is concluded then that

$$\bar{R}^n - \bar{R}_0^n = kt \quad (59)$$

with  $n$  between 2.5 and 2.75 rather than the value of  $n = 2$  concluded in the earlier paper.  $n = 2$  corresponds to the period in which the size distribution is relaxing to its steady state.

Hunderi et al.'s model (1979, 1981) is essentially deterministic as a given grain can only contact a limited number of its neighbours. In contrast, in a statistical model, such as that of Novikov (1978) and of Hillert (1965) every grain has a given probability of being in contact with all the grains in the distribution. Abbruzzese (1985) has examined the interconnections between Hillert's statistical model and the deterministic approach of Hunderi et al. in detail. In neither Hunderi et al. (1979, 1981) nor Novikov (1978) are topological constraints taken into account.

### 10.3 2-D Soap Froth Simulation

The Novikov and Hunderi et al. models refer to 3-D. Weaire and Kermode (1983, 1984) have developed a 2-D simulation of a soap froth. Their model simulates the structure and its evolution directly rather than examining a system of equations for statistical quantities as in all the models, both computer simulations and others, discussed so far. An initial structure has to be set up. In Weaire and Kermode (1983) this is an ordered hexagonal structure of equal cells, perturbed by introducing progressive changes in cell area, randomly chosen for each cell. This process is continued until one cell is about to vanish, and

then further neighbour-switching events are applied to introduce more topological disorder. This is a somewhat arbitrary procedure and Weaire and Kermode (1984) extend their initial approach and use a Voronoi network to define the initial configuration.

In the simulation, each local environment is relaxed in turn, with fixed cell areas, towards the equilibrium configuration which satisfies:-

(1) All angles at vertices equal at  $120^\circ$ .

(2) Radius of curvature of each side is

$$r = c(p_1 - p_2)^{-1} \quad (60)$$

where  $p_1$  and  $p_2$  are the pressures of the two adjacent cells and  $c$  is a constant related to the surface tension  $T$  by

$$c = 2T \quad (61)$$

If these conditions are satisfied and the gas is treated as incompressible, von Neumann's law (1952) equation (45) (as discussed in Sections 3, 9.1 and 9.4), follows from assuming that the rate of diffusion across each side is proportional to the length of that side and the pressure difference across it. The local variables Weaire and Kermode chose to relax at each step are the position of a vertex (two coordinates) and the pressures of the three surrounding cells. After the relaxation, small increments of area are transferred between the cells to simulate the growth behaviour, according to von Neumann's law. The relaxation is then repeated, and so on. From time to time, the program is required to make the elementary topological transformations of neighbour-switching and cell disappearance.

In Weaire and Kermode (1983), with the perturbed hexagonal structure starting point, the results are as follows.

(1)  $\mu_2$ , the variance in the distribution  $f_n$  of cells with  $n$  sides.

increases linearly with time (in agreement with Aboav (1980) - see earlier discussion in Section 9.2) although the times examined are relatively short.

- (2)  $f_n$  corresponds closely with that found by Aboav (1980).
- (3)  $m_n$ , the average number of sides of neighbours of an n-sided cell agrees closely with the function found by experiment (Aboav (1980)) with a value for  $\mu_2$  of 1.3.
- (4)  $\mu_2$  depends linearly on D.

For the Voronoi construction starting point, (Weaire and Kermode (1984)) the same results apply, indicating that the initial configuration is forgotten after an initial time period. It should be noted that "linear" is not a precisely tested relationship; the fluctuations in the relationships for  $\mu_2$  for instance are large. In addition, the dependence of  $f_n$  on  $\mu_2$ , and of  $f_s$  (the distribution of the length of sides) on time, show similar behaviour to Aboav (1980).  $f_A$ , (the distribution of cell areas), evolves towards a distribution which is at least roughly exponential in form:

$$f_A = \frac{1}{A} \exp\left(-\frac{A}{A}\right) \quad (62)$$

This is similar to the forms predicted by Louat (1974), by Sahni et al. (1983) (to be discussed in Section 10.5), and by Rivier (1983) (discussed in Section 9.4).

Lewis' Law, equation (42), does not hold for the simulated froth. This would appear to support the author's earlier remark (see Section 9.4) questioning Rivier's (1983) assumption that Lewis' Law applies to soap froths. According to Rivier (1985), as discussed in that section, any non-ideal random structure where an energy constraint must be invoked in addition to the minimum constraints given in (47)-(49) when applying the Maximum Entropy Formalism, will not obey Lewis' Law. This would seem to apply as much to soap froths as to metallurgical aggregates. But the question still stands as to why von

Neumann's Law, which can be derived from Lewis' Law, (Section 9.1) holds.

This brings us back to the question of the relevance of soap froths to grain growth, first discussed in Section 3. The main point to emerge is that a soap froth tends to remain in quasi-equilibrium at all times because the cell walls and enclosed gas can adjust quickly to minimize surface area, subject to the constraint of given cell areas (i.e. incompressibility of the gas) e.g. if a neighbour-switching event occurs, there will be immediate readjustment. In contrast, in polycrystals, the required changes after a neighbour-switching event will not be instantaneous. In a soap cell system, there is a sequence of equilibrium states associated with slowly changing cell areas. In grain growth in polycrystals, the problem is a kinetic one which cannot be reduced in the same way (Weaire and Kermode (1984)).

Weaire and Kermode (1984) make a very important point about the existence, or otherwise, of parabolic growth kinetics. Essentially, their comments centre around whether  $f_n$  settles down to a stable limiting form. If it does, the structure then does not change with time, in a statistical sense, and from the dimensional arguments which underlie Burke and Turnbull (1952),

$$\bar{D}^2 \sim kt$$

This must apply to both soap froths and polycrystals given a limiting form of the structure, a constant  $k$  and a single length-scale  $D$ .

However, it appears that neither system obeys the above equation. Aboav (1980) showed for 2-D soap froths  $D \sim t$ . Table 2 shows that even for high purity metals  $n \neq 2$ . For soap froths, Weaire and Kermode argue that the dimensional arguments fail because the structure itself changes with time i.e.  $\mu_2$  is dependent on  $t$ . Weaire and Kermode (1984) point out that a similar process of re-evaluation is also necessary for polycrystalline grain growth. Monte-Carlo simulations, to be discussed in Section 10.5, have begun this process (Sahni et al. (1983), Srolovitz et al. (1983), Anderson et al. (1984), Srolovitz et al. (1984b) and others) and have suggested  $D^n \sim t$  where  $n = 2.44$ , which appears to be

consistent with some of the experimental results. Weaire and Kermode, however, comment "That where the dimensional argument breaks down here is not so clear". The question which must be asked then of the Monte Carlo simulations is whether a time-varying shape distribution results. As it does not, Weaire and Kermode's explanation for deviation from parabolic kinetics fails.

Weaire and Kermode intend to go on to examine soap froth evolution in 3-D.

#### 10.4 Simulation of 2-D Grain Growth Using the Classical Boundary Migration Equation

The treatment by Ceppi and Nasello (1984) appears to be similar in spirit to that of Weaire and Kermode (1983, 1984) in that it models the structural evolution directly. In this case the boundaries move according to the classical boundary migration equation (see Section 2 for assumptions in deriving this):

$$v = \frac{K}{r} \quad (63)$$

where  $K$  is a constant and  $(1/r)$  the curvature of the boundary. They find, studying the evolution of an initially rectangular array of circular grains, that

$$\bar{D}^2 - \bar{D}_0^2 = \alpha p \quad (64)$$

where  $p$  is an adimensional parameter dependent on time. The details of their model are not clear from their short paper. In particular, they do not appear to take topological transformations explicitly into account.

## 10.5 Monte-Carlo Simulations of Grain Growth

### 10.5.1 2-D

Srolovitz et al. (1983) report a new approach (given in detail in Anderson et al (1984)) employing a Monte-Carlo simulation which allows topological constraints to be taken into account.

In the Monte-Carlo method, the microstructure is mapped onto a discrete lattice. The lattice can be triangular, square or whatever symmetry is chosen. Each lattice site is assigned a number between 1 and Q corresponding to the orientation of the grain in which it is embedded. If Q is large, grains of like orientation impinge infrequently. A grain boundary is defined to lie between sites of unlike orientation and the grain boundary energy is also specified. Sahni et al. (1983) were the first to propose the usefulness of this model for grain growth studies.

The kinetics of boundary motion are simulated by using a Monte Carlo technique. A lattice site is selected at random and a new trial orientation is also chosen at random from one of the other (Q - 1) possible orientations. The transition probability is then given by

$$W = \begin{cases} \exp(-\Delta G/k_B T) & \Delta G \geq 0 \\ 1 & \Delta G \leq 0 \end{cases} \quad \begin{matrix} (65) \\ (66) \end{matrix}$$

where  $\Delta G$  is the change in energy caused by the change in orientation,  $k_B$  the Boltzmann constant and T the absolute temperature. Successful transition at the grain boundaries to orientations of nearest neighbour grains correspond to boundary migration. The velocity  $v_i$  of a segment of the boundary is then related to the local chemical potential difference  $\Delta G_i$  by

$$v_i = \mu \left[ 1 - \exp\left(\frac{-\Delta G_i}{k_B T}\right) \right] \quad (67)$$

where  $\mu$  is the boundary mobility. The simulation process can be manipulated so that it is, if anything, only weakly dependent on the symmetry of the lattice.



For the test configuration of a circular grain embedded in an infinite matrix (i.e.  $Q = 2$ ), the grain is found to collapse symmetrically with

$$A - A_0 = -\alpha t \quad (68)$$

with  $\alpha$  a constant. The kinetics for an isolated grain are therefore parabolic, in agreement with the models discussed at the beginning of this section.

However, if an interconnected network is used the results are not parabolic. Large  $Q$  ( $Q=64$ ) and long times give grain boundary networks increasingly resembling those found in experiments. The initial state is specified by assigning a random orientation to each lattice site. The grain growth exponent is 2.44 after an initial transient.

Anderson et al (1984) discuss the deviation of the growth exponent value from the mean field, spherical grain, value of 2 in terms of the role of vertices. In continuum models, the driving force for growth is the reduction in curvature of the boundary. In lattice models, the curvature is discretized as kinks on the boundary and there are two distinct mechanisms by which these kinks can be eliminated (i.e. curvature reduced).

- (1) Meeting and annihilation of two kinks of identical orientation (as defined by the lattice) but of opposite sign.
- (2) Absorption of a kink at a vertex where more than two grains meet.

Kink elimination by the second mechanism reduces curvature without causing grain growth. Effectively, growth is slowed relative to, for example, a shrinking circular grain in an infinite matrix.

The translational and rotational degrees of freedom of a vertex become important. Vertex rotation, for instance, is capable of redistributing curvature between adjoining boundaries. Such curvature redistributions are particularly important when a grain disappears.

Since both the spatial and temporal location of disappearing grains is random and the effects of a grain disappearance are made non-local by vertex rotation, vertices introduce a randomizing (i.e. nondeterministic) aspect into grain growth. The importance of the inherent randomness in grain growth was previously appreciated by Louat (1974). This redistribution of curvature is equivalent to the Rnines and Craig (1974) propagation of topological and size changes through a structure when a grain disappears. The fact that these changes are not instantaneous is a point made by Weaire and Kermode (1984) and therefore makes the treatment of the local environment by Hunderi et al (1979, 1981) significant.

Anderson et al (1984) find that their Monte Carlo simulation growth exponent of 2.44 is in close agreement with the average exponent found in experiments with zone refined metals (although there is a wide spread between 2 and 4 - see Table 2).

The simulation is carried further in Srolovitz et al (1984). The grain size distribution function is found to be time invariant when  $R$  is scaled by  $\bar{R}$ , and fits the experimental data (Beck (1954), Aboav and Langon (1969)) better than either a log-normal function or those due to Hillert and Louat. It has a maximum at  $\sim 2.7 \bar{R}$ . The mean normalized size of  $n$ -sided grains increases linearly with  $n$  in agreement with experiment (Feltham (1957)). The topological class distribution  $f_n$  is also time-invariant, in contrast with 2-D soap froth simulations (see Sections 9.2 and 10.3) and the shape distribution predicted by Maximum Entropy considerations (Section 9.4). The mean curvature  $k$  for each individual grain is found using (for 2-D)

$$k = \frac{\pi(n-6)}{3S} \quad (69)$$

where  $S$  is the grain perimeter. The product of the curvature and the radius,  $kR$ , increases with  $n$  but the relationship is not quite linear.

It is generally observed that large grains grow and small grains shrink, but instances where the opposite is true are found. In a large number of cases, the trajectories of individual grains in radius-time

space cross, suggesting that the local environment of grains is important. In addition, a plot of  $dR/dt$  vs  $(1/R - 1/\bar{R})$  is non-linear and the noise is extremely large. If the data are replotted as  $d(R/\bar{R})/dt$  vs  $R/\bar{R}$ , the plot is virtually constant for  $(R/\bar{R}) > 1$  (see Fig. 16). Large grains are neither moving to the large  $R/\bar{R}$  nor the small  $R/\bar{R}$  sides of the distribution on average, but are randomly shrinking or growing. The magnitude of the fluctuation of the individual grain velocities, coupled with the lack of direction, suggests that these grains are executing random walks in grain-size space. On the other hand, small grains migrate rapidly towards zero grain size. This is indicative of the presence of a real directed driving force which may be equated with the curvature, which increases as  $R$  tends to zero. For large  $R$ , where the curvature is very small, the structural noise tends to randomize any directed motion.

Thus, "The true nature of grain growth lies somewhere between the concepts of curvature directed motion and random walk" state Srolovitz et al (1984). This takes us back to equation (17). The meaning of this statement is that neither term in equation (17) can be neglected.

Srolovitz et al (1984b) use the Monte Carlo simulation to examine the influence of a particle dispersion on grain growth. Grest et al (1985) study the effects of anisotropic grain boundary energies. As the anisotropy is increased, the exponent increases from 2.4 to 4, the grain size distribution functions become broader, and the microstructure consists of large grains with extended regions of small grains. Anisotropic grain boundary energies can result in preferred crystallographic orientation. Srolovitz et al (1985) have also examined abnormal grain growth using the simulation.

#### 10.5.2 3-D

The Exxon Group who have been responsible for the above studies are now embarking on the task of extending their model to 3-D. The latest paper to appear describes the beginnings of this study (Anderson et al (1985)). Addressing the correspondence between 2-D and 3-D grain growth, the grain size distribution from the 2-D simulation (Srolovitz et al (1984)) is compared with cross-sectional data from the 3-D

simulation. There is good agreement but a small discrepancy for peak height and position. Grain growth kinetics are also examined with the result:

$$\bar{V}^{0.94} - \bar{V}_0^{0.94} = kt \quad (70)$$

$$\bar{R}^{2.81} - \bar{R}_0^{2.81} = kt \quad (71)$$

Rhines and Craig (1974) found a linear dependence of  $\bar{V}$  on time and deduced that the grain growth exponent for  $\bar{R}$  should be 3, in contrast to the mean intercept dependence on time such that  $n = 2.3$ , as discussed earlier. Anderson et al (1985) comment that this must indicate that their grains are compact entities (i.e. isotropic). By implication, those of Rhines and Craig may have exhibited shape anisotropy to some extent, as concluded by the author in Section 6.

#### 11. SUMMARY

The development of grain growth theories from the early 1950's onwards has been reviewed. Burke and Turnbull (1952) suggested that the velocity of a portion of boundary should be inversely proportional to its radius of curvature and hence, using simple dimensional arguments, that grain growth should exhibit parabolic kinetics as given in equation (4). They assumed that their analysis could be extended to represent the mean behaviour of a whole array of grains but subsequent developments have proved this assumption to be inadequate.

C.S. Smith (1952) enumerated the topological requirements for space-filling in terms of the edges, faces, vertices of the ensemble. Grain growth results from the interaction between these topological requirements and the forces driving boundaries to migrate to reduce boundary curvature and hence area and energy. Thus, no grain can ever be treated as an isolated entity, as assumed by Burke and Turnbull, but must always be seen in relation to its neighbouring grains.

Feltham (1957), Hillert (1965) and Louat (1974) developed mean field theories for grain growth in which a grain is embedded in an

environment which represents the averaged effect of the ensemble of grains. Its mean growth rate can then be predicted. Feltham and Hillert took deterministic approaches, neglecting any random changes in grain size and assuming growth to occur solely as the result of the driving force for removal of boundary curvature. Louat's treatment stressed the statistical nature of growth, with boundaries executing random walks, and neglected growth due to the driving force. All these early mean field theories are thought to have given parabolic growth kinetics because they neglected topological constraints.

A neat description of grain growth as dislocation climb was presented for 2-D by Hillert (1965) and for 3-D by Morral and Ashby (1974). The dislocations were associated with grains which deviated from the average (6-sided for 2-D,  $\sim$  14-sided for 3-D). Parabolic kinetics were again derived.

Rhines and Craig (1974) suggested two new concepts, the sweep constant and the structural gradient, the latter quantifying the tendency to grain growth. The precise definition of these was the subject of debate with Doherty (1975). Doherty's definition of sweep constant  $\theta^*$  as the number of grains which vanish when boundaries sweep through a volume equal to that of the mean grain volume has been supported by Hunderi (1979). The alternative definitions for the structural gradient still stand ( $M_v/N_v$  due to Doherty (1975) and  $M_v S_v/N_v$  due to Rhines and Craig (1974)) but the evidence (e.g. Kurtz and Carpay (1980)) appears to weigh in favour of Rhines and Craig.

Rhines and Craig brought the sweep constant and the structural gradient into an algebraic analysis to obtain the grain growth kinetics taking into account topological requirements. They obtained a linear dependence of mean grain volume on time and hence a dependence of mean grain radius on  $t^{1/3}$ , rather than  $t^{1/2}$  as predicted by Burke and Turnbull (1952) and the mean field theories of Feltham (1957), Hillert (1965) and Louat (1974). They validated the  $t^{1/3}$  dependence experimentally by serial sectioning and cast doubt on the use of mean grain intercept measurements on 2-D sections. This doubt is misplaced unless the structure is anisotropic.

Blanc and Mocellin (1979) and Carnal and Mocellin (1981) have predicted the distributions of topological parameters  $f_n$  and  $m_n$  in the steady-state on the basis of the elementary topological transformations of neighbour-switching and cell disappearance.

The Rhines and Craig topological analysis for grain growth was extended by Kurtz and Carpay (1980) by dividing the grains into topological classes, each with an (assumed) log-normal distribution of grain sizes. The different classes have markedly different mean growth rates but the median diameter in each class and of the overall distribution grows parabolically. They validated their predictions experimentally and found a constant structural gradient ( $M_V S_V / N_V$ ). They suggest no explanation for the discrepancy between their  $t^{1/2}$  dependence and the  $t^{1/3}$  dependence of Rhines and Craig.

Over the last five years there have been developments in the theory of random cellular networks. Lewis' Law that the average area of an n-sided grain is linearly dependent on n has been found only to apply to ideal space-filling structures, i.e. those which satisfy Maximum Entropy considerations with the minimum of constraints (Rivier (1984)). Polycrystals are non-ideal structures and it is thought rather that the mean radius of an n-sided grain will be linearly dependent on n. Rivier (1984) finds on the basis of Maximum Entropy considerations a time-invariant size distribution but a time-variant shape distribution. This raises fundamental questions about the nature of normal grain growth i.e. does size scale but not shape? Soap froths bear some resemblance to polycrystals, although the analogy must not be pushed too far as soap froths are in quasi-equilibrium whereas polycrystals are not as solid state diffusion is slow. For soap froths, the shape distribution  $f_n$  (at least in 2-D) does broaden increasingly with time (Aboav (1980)). Experimental observations of  $f_n$  for solid polycrystals are sparse. Monte Carlo computer simulations in 2-D give a time-invariant  $f_n$ . The time dependence of  $f_n$  therefore deserves considerable attention in connection with these questions about the nature of normal grain growth.

Recently there have been a number of other computer simulation models of normal grain growth, all prompted by the general deviation of

experimental results from parabolic grain growth kinetics. Novikov (1979) assumed a log-normal size distribution of grains around each grain and calculated probabilities of certain contact areas between grains of different sizes; the approach is essentially mean field in spirit but the simulation gives a growth exponent of 2.2.

Hunderi et al. (1979a) proposed a linear bubble growth model which allowed for the effects of local environment i.e. a grain may grow in one environment where it is surrounded by smaller grains but in another may shrink as the neighbours are larger. Hunderi and Ryum (1981) extended the approach and found a growth exponent between 2.5 and 2.75. Hunderi et al's model is deterministic as a given grain can only contact a limited number of its neighbours. In contrast, in Novikov's model every grain has a given probability of being in contact with all the grains in the distribution.

Weaire and Kermode (1983, 1984) have simulated 2-D soap froth evolution directly (i.e. showing the evolution of the network over time rather than examining a system of equations for statistical quantities). Their results supported the experimental observations of Aboav (1980) that the shape distribution broadens with time.

Ceppi and Nasello have simulated 2-D grain growth using  $v \sim 1/r$ , the classical boundary migration equation. Their results are not yet sufficiently developed for comments to be made.

The most significant computer simulations to have been carried out are those already mentioned of the Exxon Group using Monte Carlo simulations (Sahni et al. (1983) Srolovitz et al. (1983), Anderson et al. (1984), Srolovitz et al. (1984)). Topological constraints are an inherent part of the model. The network is simulated directly as in the Weaire and Kermode soap froth model. Anderson et al. (1984) identifies the absorption of curvature by vertices without the curvature causing grain growth as a mechanism by which the growth exponent is increased above 2 relative to the mean field theories. The grain growth exponent found for 2-D is 2.44, which agrees well with the average from experiment. Srolovitz et al (1984) examine the trajectories of individual grains in grain-size time space. Large grains tend to

exhibit random walks. Small grains migrate rapidly towards zero grain size as under the driving force of the curvature. For large grains, the curvature is small and directed motion tends to be randomized. They conclude "the true nature of grain growth lies somewhere between the concepts of curvature directed motion and random walk". This statement achieves a vital link with equation (17) which is the basis of the mean field theories of Feltham (1957), Hillert (1965) and Louat (1974), i.e. diffusion and directed motion are both important, neither term can be neglected. An analytical solution for (17) has never been attempted and may not be possible. Computer simulation has therefore played a key role in providing insight into grain growth and its theoretical framework. The ramifications of the Srolovitz et al (1984) conclusion have yet to be explored in depth.

#### ACKNOWLEDGEMENTS

I would like to thank Mr. A.D. Le Claire, Professor A. Rabinovitch and Dr. A.M. Stoneham for stimulating discussions and for helpful comments on the manuscript.

#### REFERENCES

- Abbruzzese, G., *Acta. Met.*, 33 No. 7 (1985) 1329-1337.
- Aboav, D.A., *Metallography*, 3 (1970) 383-390.
- Aboav, D.A., *Metallography*, 4 (1971) 425-441.
- Aboav, D.A., *Metallography*, 13 (1980) 43-58.
- Aboav, D.A. and Langdon, T.G., *Metallography*, 2 (1969) 171-178.
- Anderson, M.P., p. 15-34 in "Annealing processes - Recovery, recrystallisation and grain growth", Editors, Hansen, N., Jensen, D. Juul, Leffers, T. and Ralph, B., 7th International Risø Symposium on Metallurgy and Materials Science, 1986.
- Anderson, M.P., Grest, G.S. and Srolovitz, D.J., *Scripta. Met.*, 19 (1985) 225-230.
- Anderson, M.P., Srolovitz, D.J., Grest, G.S. and Sahri, P.S., *Acta. Met.*, 32 No. 5 (1984) 783-791.
- Ashby, M.F. and Verrall, R.A., *Acta. Met.*, 21 (1973) 149-163.



- Bauer, Ch.L., J. de Physique, Colloque C6, Supplement to No. 12, 43 (1982) C6-187.
- Beck, P.A., Phil. Mag. Suppl., 3 (1954) 245.
- Blanc, M. and Mocellin, A., Acta. Met., 27 (1979) 1231-1237.
- Bolling, G.F. and Winegard, W.C., Acta. Met., 6 (1958) 283-287.
- Burke, J.E. and Turnbull, D., Prog. Metal Physics, 3 (1952) 220-292, Ed. Chalmers, B., Pergamon.
- Cahn, R.W., Nature, 250 (1974) 702-703.
- Cahn, J.W. and Padawer, G.E., Acta. Met. 13 (1965) 1091-1092.
- Carnal, E. and Mocellin, A., Acta. Met., 29 (1981) 135-143.
- Ceppi, E.A. and Nasello, O.B., Scripta. Met., 18 (1984) 1221-1225.
- Doherty, R.D., Met. Trans., 6A (1975) 588-590.
- Doherty, R.D. J. Materials Education, 6 (1984) 841-883.
- Drolet, J.P. and Galibois, A., Acta. Met., 16 (1968) 1387-1399.
- Feltham, P., Acta. Met., 5 (1957) 97.
- Fortes, M.A., Acta. Met., 34 No. 1 (1986) 33-36.
- Fortes, M.A. and Ferro, A.C., Acta. Met., 33 No. 9 (1985) 1683-1696.
- Fortes, M.A. and Ferro, A.C., Acta. Met., 33 No. 9 (1985) 1697-1708.
- Gordon, P. and Bassyouni, T.A.El., Trans. Am. Inst. Min. Engrs., 233 (1965) 391-397.
- Grest, G.S., Srolovitz, D.J. and Anderson, M.P., Acta. Met., 33 No. 3 (1985) 509-520.
- Grey, E.A. and Higgins, G.T., Scripta Met., 6 (1972) 253-?
- Grey, E.A. and Higgins, G.T., Acta. Met., 21 (1973) 309-?
- Hillert, M., Acta. Met., 13 (1965) 227-238.
- Holmes, E.L. and Winegard, W.C., Acta. Met., 7 (1959) 411-414.
- Hu, H., Can. Met. Quart., 13 (1974) 275-286.
- Hunderi, O., Acta. Met., 27 (1979) 167-169.
- Hunderi, O. and Ryum, N., J. Mat. Sci., 15 (1980) 1104-1108.

- Hunderi, O. and Ryum, N., *Acta. Met.*, 29 (1981) 1737-1745.
- Hunderi, O., Ryum, N. and Westengen, H., *Acta. Met.*, 27 (1979) 161-165.
- Kikuchi, R., *J. Chemical Physics*, 24 No. 4 (1956) 861-867.
- Kurtz, S.K. and Carpay, F.M.A., *J. Appl. Phys.*, 51 No. 11 (1980a) 5725-5744.
- Kurtz, S.K. and Carpay, F.M.A., *J. Appl. Phys.*, 51 No. 11 (1980b) 5745-5754.
- Lambert, C.J. and Weaire, D., *Phil. Mag.*, B47 No. 4 (1983) 445-450.
- Lantuejoul, C., *Lecture Notes in Biomathematics*, 23 (1978) 323-329.
- Lewis, D., *Anatom. Rec.*, 38 No. 3 (1928) 351.
- Louat, N.P., *Acta. Met.*, 22 (1974) 721-724.
- Martin, J.W. and Doherty, R.D., p. 228 in "Stability of microstructure in metallic systems", Published Cambridge University Press, (1976).
- Morral, J.E. and Ashby, M.F., *Acta. Met.*, 22 (1974) 567-575.
- Novikov, V.Yu., *Acta. Met.*, 26 (1978) 1739-1744.
- Novikov, V.Yu., *Acta. Met.*, 27 (1979) 1461-1466.
- Rhines, F.N. and Craig, K.R., *Met. Trans.*, 5 (1974) 413-425.
- Rhines, F.N. and Craig, K.R., *Met. Trans.*, 6A (1975) 590-591.
- Rhines, F.N. and Patterson, B.R., *Met. Trans.*, 13A (1982) 985-993.
- Rivier, N., *Phil. Mag.*, B47 No. 5 (1983) L45-L49.
- Rivier, N., *Phil. Mag.*, B52 No. 3 (1985) 795-819.
- Rivier, N. and Lissowski, A., *J. Phys. A: Math. Gen.*, 15 (1982) L143-L148.
- Simpson, C.J., Beingsner, C.J. and Winegard, W.C., *Trans. AIME*, 239 (1967) 587.
- Smith, C.S., "Metal Interfaces", ASM, (Cleveland, Ohio) (1952) 65-113.
- Smith, C.S., *Trans. A.S.M.*, 45 (1953) 533-575.
- Smith, C.S., *Scientific American*, 190 (1954) 58-64.
- Smith, C.S., *Rev. Mod. Phys.*, (April 1964) 524-532.
- Smith, C.S., *Metallurgical Reviews*, 9 (1964b) 1-48.

- Srolovitz, D.J., Anderson, M.P., Grest, G.S. and Sahni, P.S., *Scripta. Met.*, 17 (1983) 241-246.
- Srolovitz., D.J., Anderson, M.P., Grest, G.S. and Sahni, P.S., *Acta. Met.*, 32 No. 9 (1984a) 1429-1438.
- Srolovitz., D.J., Anderson, M.P., Sahni, P.S. and Grest, G.S., *Acta. Met.*, 32 No. 5 (1984b) 793-802.
- Srolovitz., D.J., Grest, G.S. and Anderson, M.P., *Acta. Met.*, 33 No. 12, (1985) 2233-2247.
- Underwood, E.E., "Quantitative Stereology", Addison-Wesley, (Massachusetts) (1970).
- Von Neumann, J., "Metal Interfaces", ASM (Cleveland, Ohio) (1952) 108-110.
- Weaire, D., *Metallography*, 7 (1974) 157-160.
- Weaire, D. and Kermode, J.P., *Phil. Mag.*, B47 No. 3 (1983a) L29-L31.
- Weaire, D. and Kermode, J.P., *Phil. Mag.*, B48 No. 3 (1983b) 245-259.
- Weaire, D. and Kermode, J.P., *Phil. Mag.*, B50 No. 3 (1984) 379-395.
- Weaire, D. and Rivier, N., *Contemp. Phys.*, 25 No. 1 (1984) 59-99.

Table 1

Kinetics of grain growth for various mechanisms (from Brook (1976))

	n in $G_c \propto t^{\frac{1}{n}}$
<b>Pore Control:</b>	
Surface Diffusion	4
Lattice Diffusion	3
Vapour Transport (P = const)	3
Vapour Transport (P = 2S/r)	2
<b>Boundary Control:</b>	
Pure System	2
Impure System:	
Coalescence of second phase by lattice diffusion	3
Coalescence of second phase by grain boundary diffusion	4
Solution of second phase	1
Diffusion through continuous second phase	3
Impurity drag (low solubility)	3
Impurity drag (high solubility)	2

Table 2

Grain growth exponents for isothermal grain growth in metals  
(from Anderson et al (1984))

<u>Metal</u> (Zone-Refined)	<u>Exponent, n</u>	<u>Reference</u>
Al	4	Gordon and Bassyouni (1965)
Fe	2.5*	Hu (1974)
Pb	2.5	Bolling and Winegard (1958)
Pb	2.4	Drolet and Galibois (1968)
Sn	2.3	Drolet and Galibois (1968)
Sn	2	Holmes and Winegard (1959)

\* This exponent was observed to vary with test temperature range.

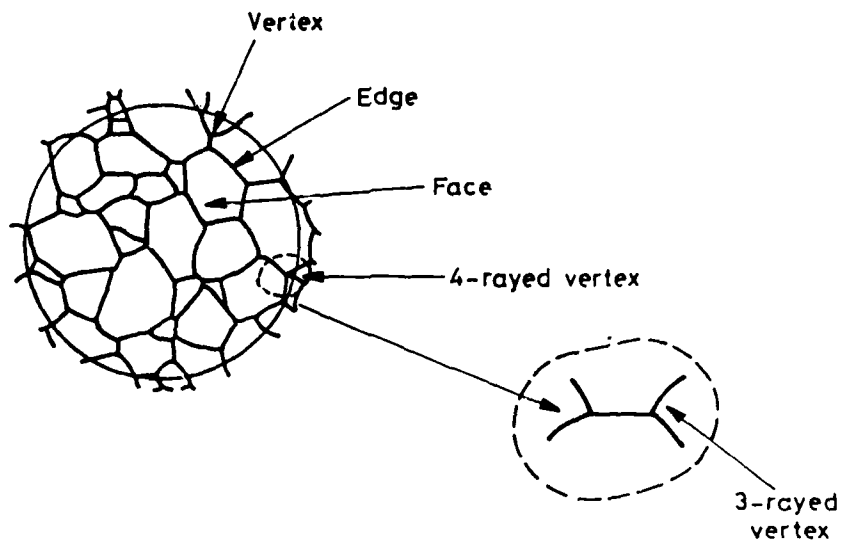


Fig. 1 Typical 2-D Section through a 3-D Grain Structure (After Underwood (1970)). The 4-Rayed Vertex will tend to Decompose into Two Three-Rayed Vertices as Growth Occurs.

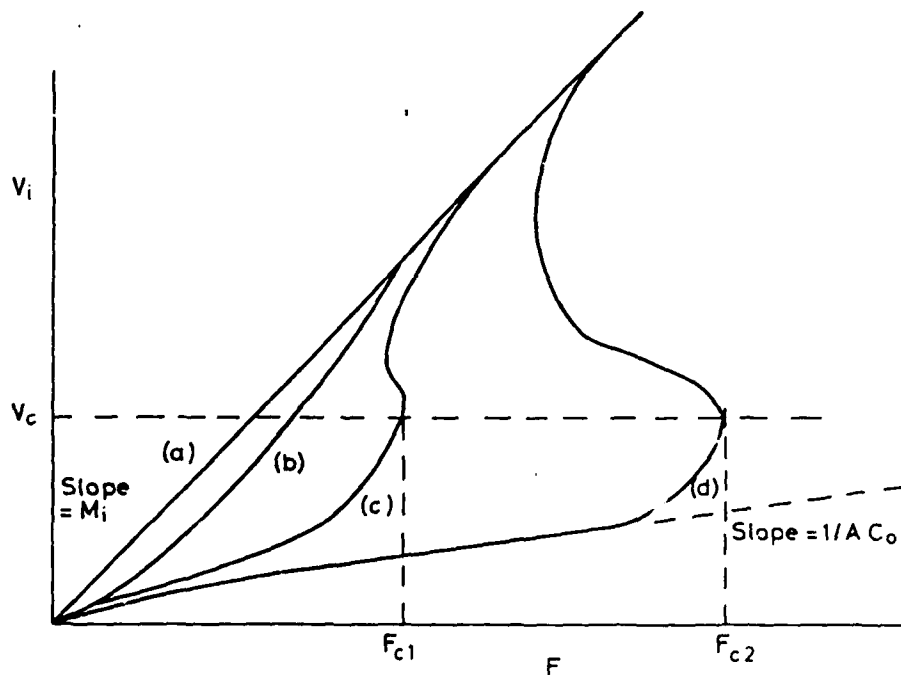


Fig.2 Schematic Representation of Grain Boundary Velocity  $v_i$  as a Function of Driving Force for (a) Pure Material (b) Impure Material not Exhibiting Breakaway. (c) Impure Material Exhibiting Breakaway at  $F_{c1}$  (d) Highly Impure Material Exhibiting Breakaway at  $F_{c2}$  (from Bauer (1982)).

Breakaway occurs at constant critical velocity  $v_c$  and limiting slopes (mobilities) are given by

$$M = \frac{M_i}{1 + M_i A C_0}$$

The slope reduces to  $M_i$  and  $1/A C_0$  for the intrinsic and extrinsic cases respectively.

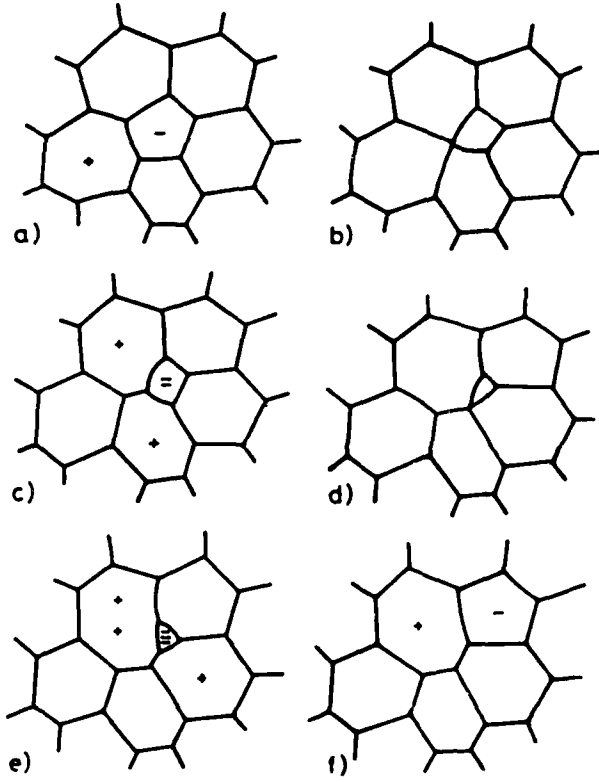


Fig. 3 2-D Grain Structure Illustrating Instability when the Array does not Consist only of Regular Hexagons (after Hillert (1965)).



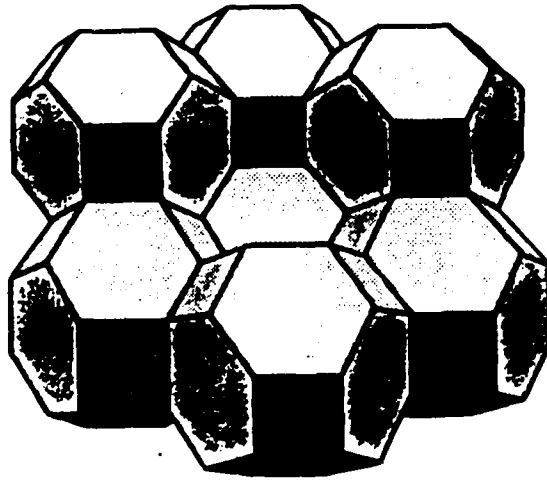


Fig. 4 A Group of Regular Tetrakaidecahedra  
(after Smith (1952)).

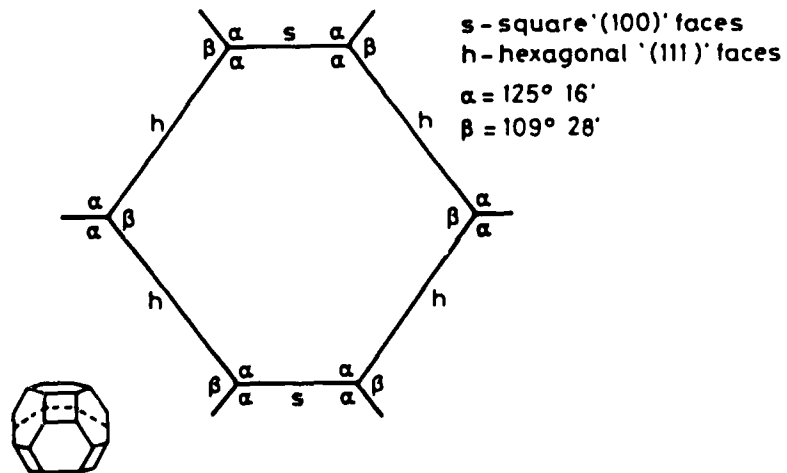


Fig. 5 Section through a Tetrakaidecahedron showing the  
Deviation from Equilibrium Angles (after Doherty (1984))

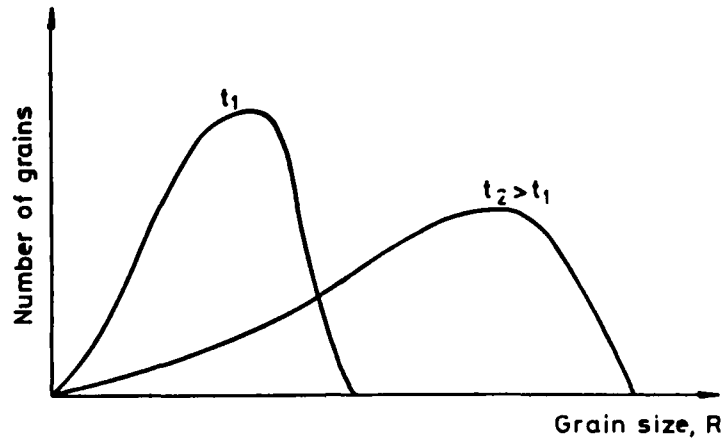


Fig 6(a) Number of Grains Versus Grain Size at Increasing Time  $t$ .

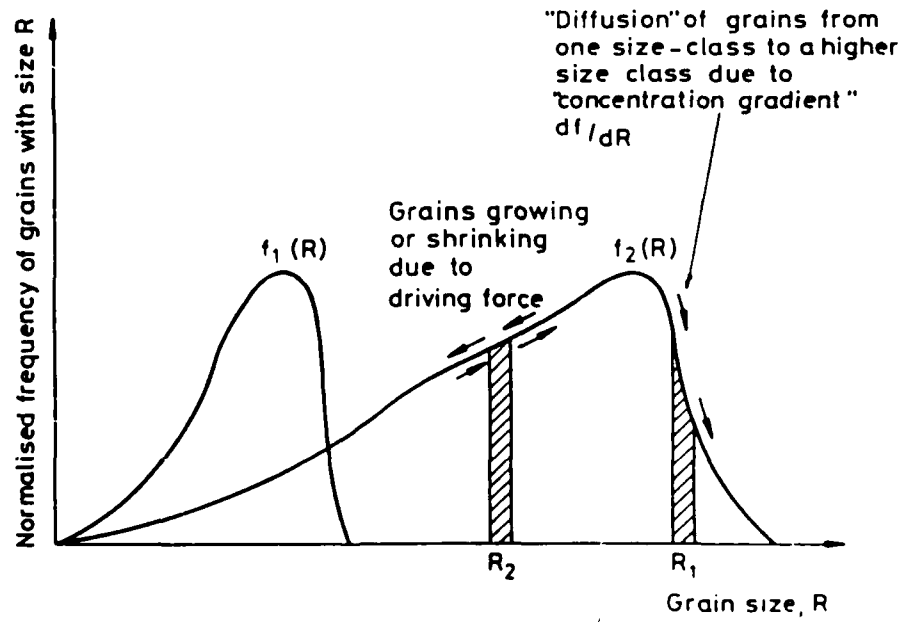


Fig. 6(b) Grain Size Distributions.

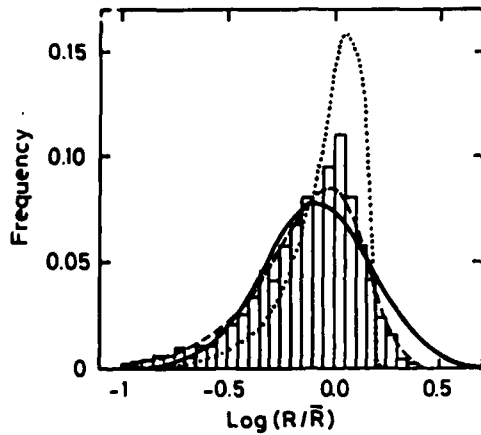


Fig. 7(a) The Grain Size Distribution Function from Computer Simulation (Histogram) (see Section 10.4) Compared with Three Theoretical Distributions: the Log-Normal (Solid) and those Proposed by Hillert (1965) (Dotted) and Louat (1974) (Dashed) (After Srolovitz et al (1984)).

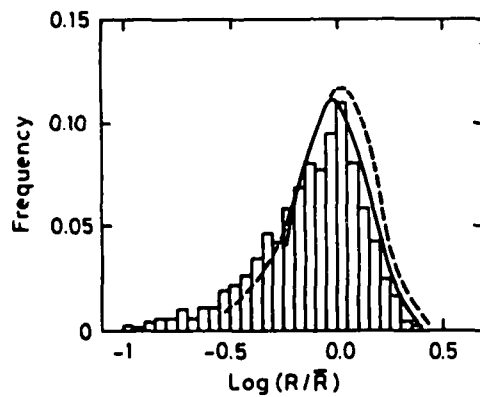


Fig. 7(b) The Grain Size Distribution Function from Computer Simulation (Histogram) (see Section 10.4) Compared with a Log-Normal fit to Experimental Data of Beck (1954) for Al (Solid Curve) and Aboav and Langdon (1969) for Mg O (Dashed Curve) (After Srolovitz et al (1984)).

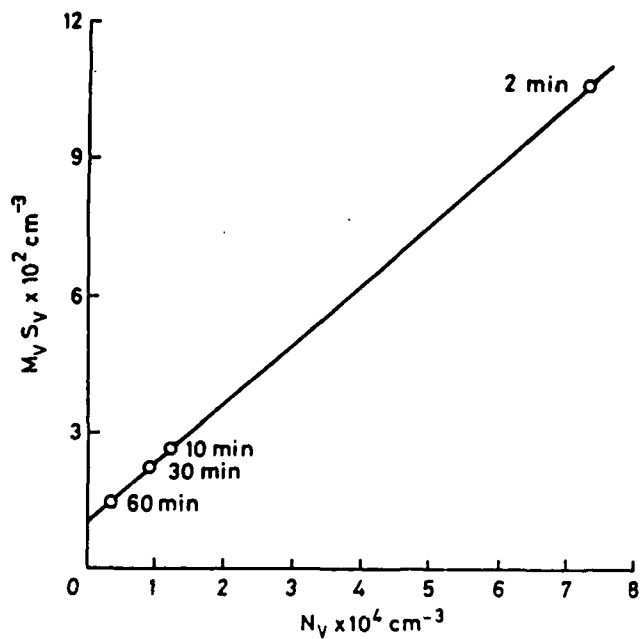


Fig. 8. Plot of  $M_V S_V$  Versus  $N_V$  for Steady State Grain Growth in Al. (After Rhines and Craig (1974))

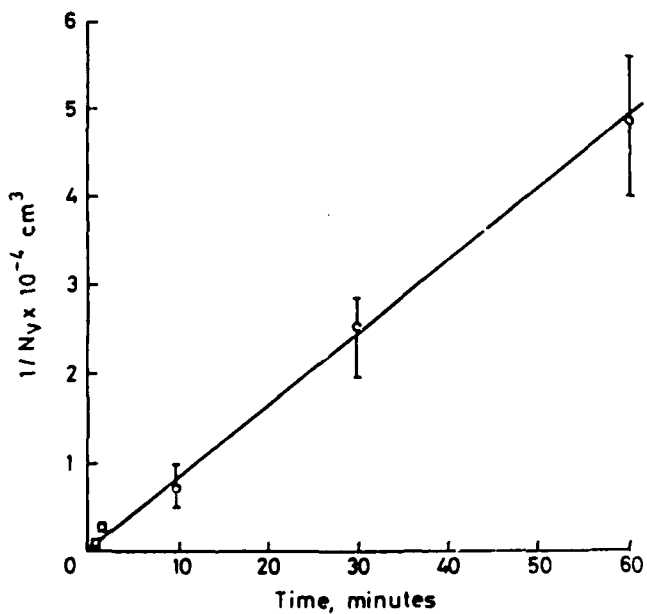


Fig. 9 Plot of Grain Volume ( $1/N_V$ ) Against Time of Annealing for Aluminium Showing a Linear Relationship (After Rhines and Craig (1974)).

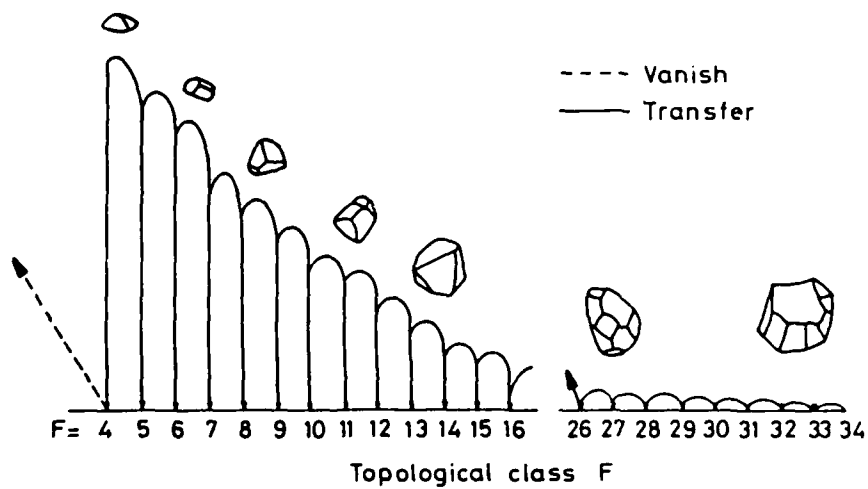


Fig. 10 Schematic Representation of Grain Transfer Between Topological Classes in a Fixed Time Interval. The Transfer of Larger Grains to the Next Lower Class Results in a Continuous Growth of the Mean Diameter in the Classes with  $F < \bar{F}$  even Though all the Individual Grains in These Classes are Collapsing due to Surface Tension Constraints. The Transfer Rates are Greatest in the Lowest Classes. (After Kurtz and Carpay (1980)).

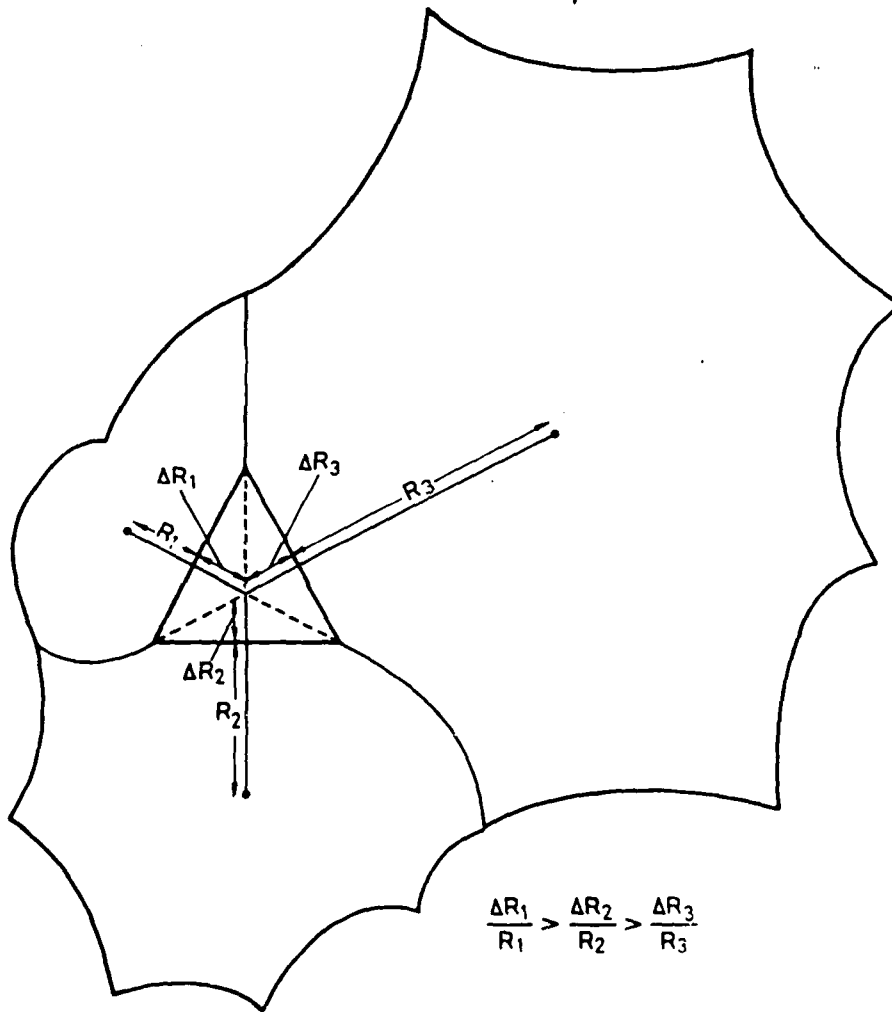


Fig. 11 Schematic Diagram Illustrating that as a 3-sided Grain Shrinks Adjacent Grain Gain in Diameter in Inverse Proportion to their Diameter

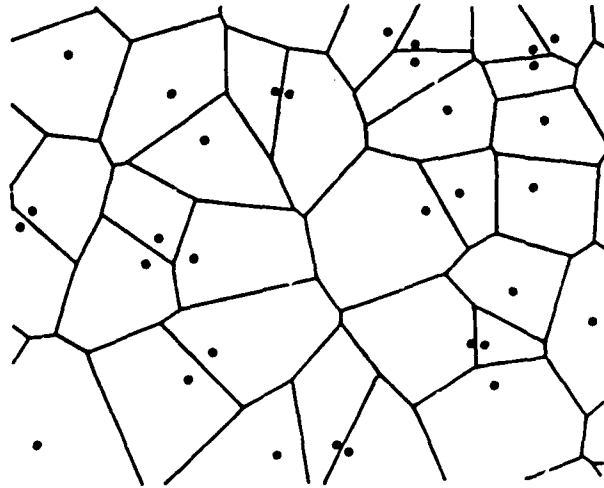


Fig. 12 Voronoi Construction for Random Points  
(After Weaire and Rivier (1984)).

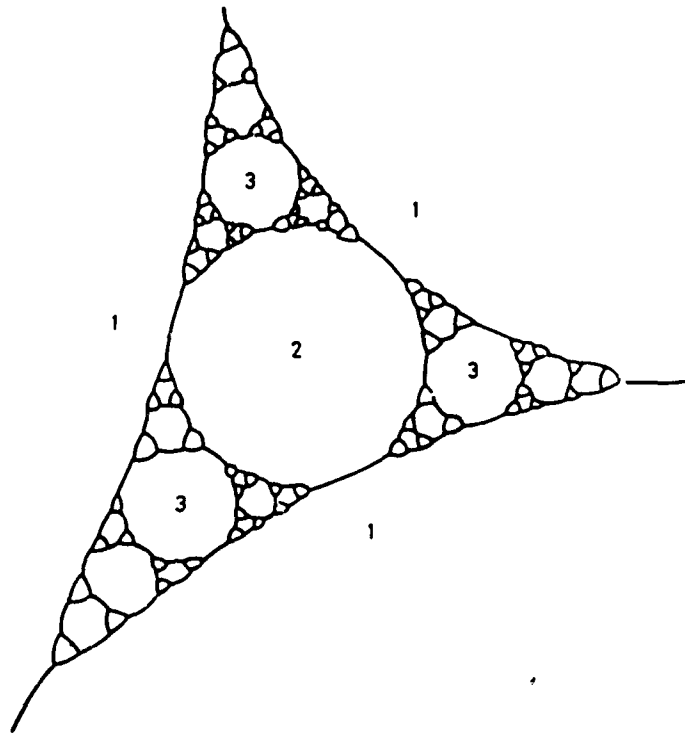


Fig. 13 Illustration of a Fractal Structure for a Soap Cell  
System (After Weaire and Rivier (1984)).

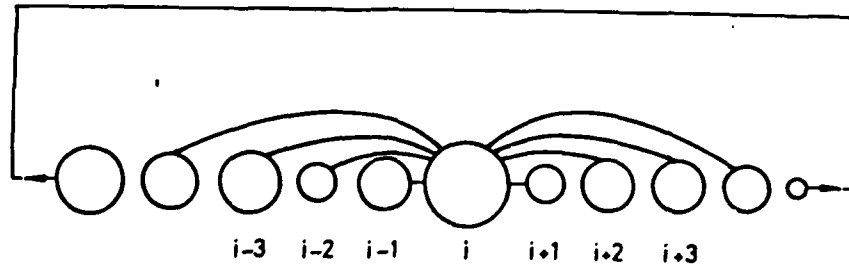


Fig. 14 The Generalised Grain Growth Model in Hunderi and Ryum (1979). Only Contacts Activated from Grain  $i$  are Shown. The Process is Repeated for all Grains

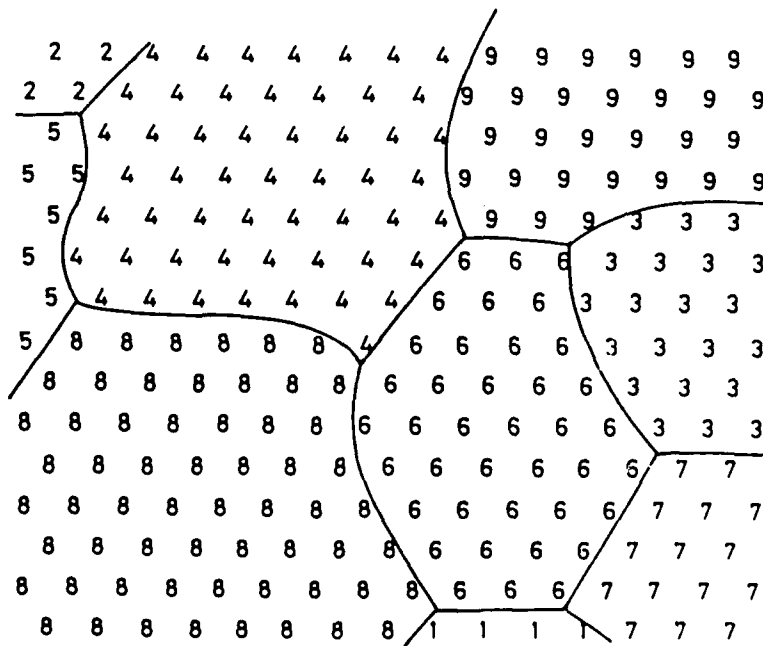


Fig. 15 Sample Microstructure on a Triangular Lattice where Integers Denote Orientation and Lines Represent Grain Boundaries (after Anderson et al (1984)).



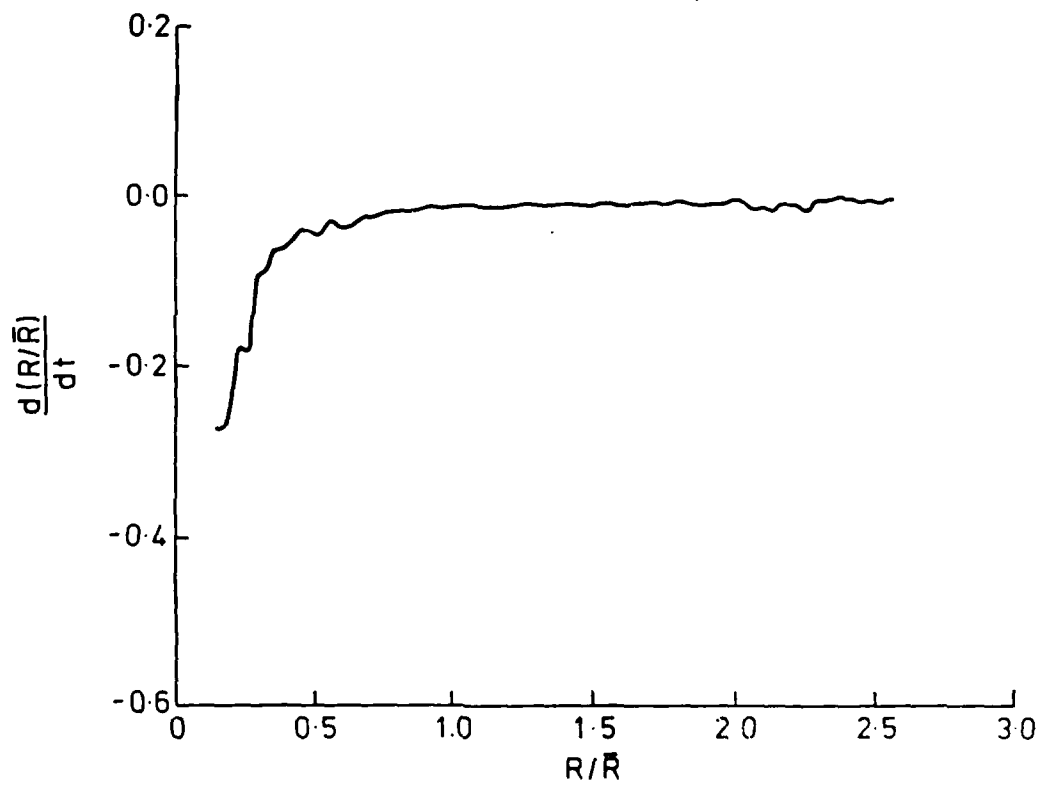


Fig. 16. The Growth Rate of Individual Grains in Normalized Grain Size Space,  $d(R/\bar{R})/dt$  Versus  $R/\bar{R}$ . (After Srolovitz et al (1984))

**END**  
**FILMED APRIL 1987**

END

DATE

~~FILMED~~

4 88

DTIC